# CALCIUM ALLEVIATES SYMPTOMS IN HYPERKALEMIC PERIODIC PARALYSIS BY REDUCING THE ABNORMAL SODIUM INFLUX

By: Danica DeJong

This thesis is submitted as a partial fulfillment of the M.Sc program in Cellular and Molecular Medicine

University of Ottawa

June 30th, 2012

# ABSTRACT

Hyperkalemic periodic paralysis, HyperKPP, is an inherited progressive disorder of the muscles caused by mutations in the voltage gated sodium channel ($Na_V1.4$). The objectives of this thesis were to develop a technique for measurement symptoms *in vivo* using electromyography (EMG) and to determine the mechanism by which $Ca^{2+}$ alleviates HyperKPP symptoms, since this is unknown. Increasing extracellular $[Ca^{2+}]$ ($[Ca^{2+}]_e$) from 1.3 to 4 mM did not result in any increases in $^{45}Ca^{2+}$ influx suggesting no increase in intracellular $[Ca^{2+}]$ ($[Ca^{2+}]_i$) acting on an intracellular signaling pathway or on an ion channel such as the $Ca^{2+}$sensitive $K^+$ channels. HyperKPP muscles have larger TTX-sensitive $^{22}Na^+$ influx than wild type muscles because of the defective Nav1.4 channels. When $[Ca^{2+}]$ was increased from 1.3 to 4 mM, the abnormal $^{22}Na^+$ influx was completely abolished. Thus, one mechanism by which $Ca^{2+}$alleviates HyperKPP symptoms is by reducing the abnormal $Na^+$ influx caused by the mutation in the $Na_V1.4$ channel.

# TABLE OF CONTENTS

# LIST OF FIGURES

# LIST OF TABLES

# LIST OF ABBREVIATIONS

| | |
|---|---|
| $[\ ]_I$ | intracellular concentration |
| $[\ ]_e$ | extracellular concentration |
| °C | degree Celsius |
| ANOVA | analysis of variance |
| AP | action potential |
| BK | big potassium channel |
| $Ca^{2+}$ | calcium ion |
| $Ca_V1.1$ | L-type calcium channel |
| $Cl^-$ | chloride ion |
| ClC-1 | chloride channel |
| DHPR | dihydropyridine receptor |
| EDL | extensor digitorum longus |
| $E_m$ | resting membrane potential |
| EMG | electromyography |
| $E_{rev}$ | Reversal potential |
| FDB | Flexor digitalis brevum |
| g | grams |
| $G_{Na}$ | sodium conductance |
| HyperKPP | hyperkalemic periodic paralysis |
| Hz | hertz |
| $K^+$ | potassium ion |
| $K_{ATP}$ channel | ATP – sensitive $K^+$ channel |
| $K_{ir}$ | inward rectifying potassium channel |

| | |
|---|---|
| $K_V$ | voltage sensitive $K^+$ channel |
| min | minutes |
| mg | milligram |
| $Mg^{2+}$ | magnesium ion |
| mM | millimolar |
| mm | millimeter |
| mL | milliliter |
| ms | millisecond |
| mV | millivolt |
| n | number of samples |
| $Na^+$ | sodium ion |
| $Na_V$ | voltage gated sodium channel |
| $N/cm^2$ | Newton per centimeter squared |
| nmol | nano moles |
| nM | nanomolar |
| PAM | potassium aggravated myotonia |
| RyR | Ryanodine receptor |
| SE | standard error |
| sec | seconds |
| SR | sarcoplasmic reticulum |
| TTX | tetrodotoxin |
| µCi | micro curies |
| µmol | micro moles |
| µV | microvolts |
| WT | wild type |

# CHAPTER 1: INTRODUCTION

Contraction in skeletal muscle is initiated by motor neurons which innervate muscles. The action potential (AP) generated in motor neuron travels to the synapse between the nerve and the muscle fiber, called the neuromuscular junction. At the neuromuscular junction, the motor neuron releases the neurotransmitter acetylcholine. The acetylcholine acts on acetylcholine gated cation channels in the muscle fiber membrane, causing them to open. This allows large quantities of sodium to enter the muscle cell, causing a depolarization large enough to activate voltage gated $Na^+$ channels ($Na_V$), initiating the AP in the muscle fiber. These action potentials propagate all along the surface of the membrane, and down into the t-tubules. Once the action potential reaches the t – tubules, the sarcoplasmic reticulum becomes activated and releases $Ca^{2+}$ into the extracellular space. The $Ca^{2+}$ ions then activate the contractile apparatus of the muscle fiber, which ultimately gives rise to the muscle contraction.

The action potential is generated through careful manipulation of ion channels and transporters found in the cell membrane as well as through the use of electrochemical gradients. In addition, in order for the action potential to propagate along the surface of the muscle, the resting membrane potential must be maintained. The resting membrane potential is maintained through regulation of the permeability of ions across the membrane, keeping the inside of the cell more negative than the outside. The normal resting membrane potential is about – 80 mV. The ion channels predominantly responsible for maintenance of the membrane potential are the chloride and potassium channels. The channel that is mainly involved in the generation of the action potential is the voltage gated sodium channel ($Na_V1.4$), which is responsible for the depolarisation of the membrane. The voltage sensitive $K^+$ ($K_V$) channel is responsible for the repolarisation phase of the action potential.

There are several disorders caused by a mutation in any one of the ion channels responsible for the maintenance of resting membrane potential and the generation of the action potential. These disorders are called channelopathies. One such disorder, Hyperkalemic Periodic Paralysis (HyperKPP), is caused by one of several mutations to the $Na_V1.4$. The symptoms of HyperKPP include, as the name suggests, intermittent episodes of paralysis, coupled with myotonic discharges that occur between and during the paralytic attacks. HyperKPP predominantly affects limb muscles, and does not affect the diaphragm muscle. Patients experiencing paralysis are completely immobilized for the duration of the attack, which is variable, and can last anywhere from a few hours to multiple days in duration. Most patients experience their first paralytic attack in the first decade of their lives, with an increasing frequency and severity of attacks through adolescence and early adulthood. This progresses to middle age where the frequency of attacks lessens, but patients are left with a vacuolar myopathy that leaves many requiring assistive devices for mobility. There is a high degree of variability in the presentation of the disease both between and within patients. As the name of the disorder suggests, the blood serum levels of $K^+$ are elevated during a paralytic attack. Patients with HyperKPP are hypersensitive to $K^+$, and ingestion of $K^+$ remains one of the most consistent triggers for paralysis. Other triggers include a period of rest following exercise, cold exposure, fasting and emotional stress.

There are very few treatment options for patients with HyperKPP. Currently the only interventions for these patients include the carbonic anhydrase inhibitor acetazolamide, which reduces the frequency of the paralytic attacks, salbutamol and calcium gluconate. However, acetazolamide is not effective in all cases, and becomes ineffective over time in the majority of patients (Bradley et al., 1990, Lehmann-Horn 2007, Pearson, 1964, Streeten et al., 1971). Salbutamol is promising in short term studies, but quickly loses its efficacy. Administration of calcium gluconate has been shown to reduce the severity of the paralytic attacks (Gamstrop et al., 1957, Pearson, 1964). At this time, the mechanism through which the calcium is benefitting these patients is unknown, and is the focus of this study. In order to develop more effective treatments for HyperKPP, we must first understand the mechanism through which $Ca^{2+}$ alleviates symptoms, so that we can exploit this mechanism with new treatments.

### 1.1 - MUSCLE CONTRACTION ANDMEMBRANE POTENTIALS

In skeletal muscle, action potentials cause a release of $Ca^{2+}$ which then activates the contractile apparatus (Vilin and Ruben, 2001). First, the action potential propagates along the sarcolemma and down the t–tubules. The depolarisation of the t-tubular membrane activates L-type $Ca^{2+}$ calcium channels, also known as dihydropyridine receptors (DHPR).These channels physically interact with the ryanodine receptors (RYRs), which are the $Ca^{2+}$ release channels of the sarcoplasmic reticulum (SR).Upon activation of the L-type $Ca^{2+}$ channels, the RYRs also become activated causing the release of $Ca^{2+}$ from the SR into the myoplasm (Nakai et al., 1998 (2)).The subsequent increase in intracellular [$Ca^{2+}$] ($[Ca^{2+}]_i$), begins the cascade of events which leads to contraction. $Ca^{2+}$bind to troponin C.  Troponin C is bound to the actin or thin filaments. $Ca^{2+}$causes a conformational change which causes it to 'tug' on tropomysin, which in turn moves the tropomyosin, uncovering the myosin binding sites on actin. The myosin then pulls on the actin, causing shortening of the muscle. To end the contraction, $Ca^{2+}$detaches from troponin, and the myosin and actin become relaxed. $Ca^{2+}$is pumped into the SR by way of $Ca^{2+}$-ATPases.

The membrane potential ($E_m$) is tightly regulated in muscle fibers. $E_m$ is produced by concentration gradients and permeabilities of ions on each side of the membrane. In addition, there are several pumps in the cell membrane that affect $E_m$, for example, the $Na^+$ - $K^+$ ATPase. There are two main factors involved in determining the movement of ions: the concentration gradient and the electrical gradient. The different concentration gradients are the first driving force behind ion movement across the cell membrane. Typically, there is a much greater concentration of $Na^+$ and $Cl^-$ outside of the cell while $K^+$ has a greater concentration inside. In order to contribute to $E_m$, there must be net movement of ions across the membrane. At rest, $Na^+$ permeability is very small and thus does not contribute to $E_m$. $K^+$ is important for the maintenance of $E_m$, as the membrane is permeable to $K^+$ at -80 mV. According to the concentration gradient, $K^+$ has a tendency to leave the cell, as the intracellular $[K^+]$, $[K^+]_i$, is higher than the extracellular $[K^+]$, $[K^+]_e$. $Cl^-$ has a large role in the maintenance of $E_m$, since the membrane is also permeable to $Cl^-$. In the case of $Cl^-$, there is a higher $[Cl^-]_e$, so according to the concentration gradient alone, $Cl^-$ enters the cell. However, the membrane potential is complex, and the concentration gradient is not the only factor involved.

In addition to the concentration gradient influencing the movement of ions across the membrane, there is also an electrical gradient. The electrical gradient exists because the inside of the cell is much more negative than the surrounding medium. For each ion, there is a given membrane potential where there would be no net movement of that particular ion. This is called the reversal or equilibrium potential. In the case of the muscle cell membrane, there are several ions involved, each with their own reversal potentials. The $E_{rev}$ for each ion is: +60 mV for $Na^+$ ($E_{Na}$), -90 mV for $K^+$ ($E_K$) and -66 mV for $Cl^-$ ($E_{Cl}$) (Begenisich and Cahalan, 1980). Typically, $E_m$ for a skeletal muscle cell is around -80 mV. Each ion is trying to bring $E_m$ towards its own equilibrium, which leads to constant ion flux. $K^+$ tends to leave the cell, since $E_K$ at -90 mV is more negative than $E_m$. The $K^+$ channels that tend to be open at rest are the $K_{ir}2.1$, a strong inward rectifier, and the $K_{ATP}$ channel.(Fakler et al., 1995). $Cl^-$ also tends to leave the cell, since $E_{Cl}$ is -66 mV, which is less negative than $E_m$. The channel responsible for the movement of $Cl^-$ ions is the ClC-1 chloride channel, which tends to be open at rest. $Na^+$ would tend to enter the cell, since $E_{Na}$ is +60 mV, however, as previously mentioned, the $Na_V1.4$ is closed at -80 mV, so $Na^+$ has a very low net flux.

Action potentials, short events during which $E_m$ is rapidly depolarized and then repolarised, are responsible for transmitting the electrical signal in muscles. In skeletal muscle, action potentials are generated when the membrane is depolarized to about –60 mV. Once this threshold is reached, a cascade of events begins that results in the reversal of $E_m$ to +30 mV. The action potential is largely generated by the $Na_V1.4$ in the skeletal muscle (Vilin and Ruben, 2001). $Na_V1.4$ channels are responsible for the depolarization phase of the action potential, the phase in which the membrane potential becomes increasingly positive, as well as the propagation of the action potential (See fig 1.1). The depolarisation phase of the action potential is terminated when the inactivation of the $Na_V1.4$ channels occurs. This greatly reduces $Na^+$ influx due to the large decrease in $Na^+$ permeability. Also at this time, $K_V$ channels become activated to allow $K^+$ to efflux from the cell, which begins the repolarisation phase of the action potential. During the repolarisation phase, $E_m$is returned to -80 mV to terminate the action potential (Vilin and Ruben, 2001).

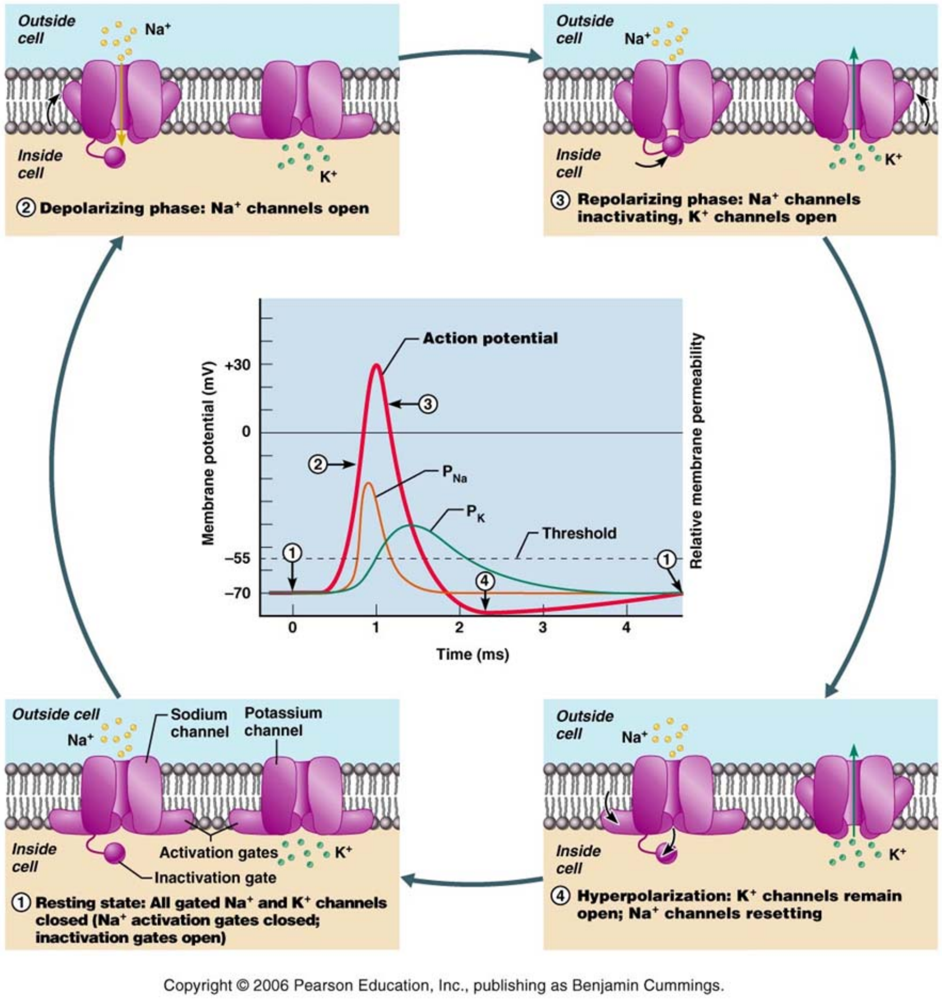


**Figure 1.1: The action potential cycle**. In the center, the action potential and the ion fluxes that occur. Around the outside – schematics of the NaV and Kv channels, describing the sequence of events that leads from resting state to full depolarization and back to repolarisation. From Marieb and Hoehn, 2006.

## 1.2 - THE VOLTAGE GATED SODIUM CHANNEL: $Na_V$1.4:

*Electrophysiology of the $Na_V$1.4: Activation, Deactivation, and Inactivation*

When discussing the $Na_V$ channel, there are three possible states in which the channel can exist: activated, deactivated or inactivated. Activation of the $Na_V$ channel occurs when threshold (-60 mV) has been reached, and simply means that the channel is opening. Activation is a highly voltage dependant process. When considering the steady state I-V curve (current-voltage relationship) it is evident that there is some current through the $Na_V$1.4 beginning at -60mV, and the current reaches a maximum at about -10 mV , with about 50% of the channels open at – 30 mV (Rojas et al., 1999)(See fig 1-2). When resting membranes are exposed to TTX, a blocker of the $Na_V$1.4 channel, there is a slight hyperpolarisation of the membrane (Yensen et al., 2002**).**Therefore, there is a very slight permeability to $Na^+$ at resting $E_m$. However, this reaffirms that there is very little permeability of $Na^+$ at the resting potential of -80 mV, as there is only a very slight change in $E_m$ when the $Na^+$ channels are blocked.

During the action potential, each channel is only open for a fraction of a second. It is the summation of all of the $Na_V$1.4 channels in the membrane that causes the characteristic shape of the action potential, as each channel opens when it becomes activated according to the steady state I – V curve. The total $Na^+$ current begins to decrease as $E_m$ becomes more and more positive. The process responsible for the closing of the channels while the $E_m$ is at or above threshold in order to end the rise phase of the action potential is fast inactivation. This allows for the repolarisation of the membrane. Fast inactivation occurs over a period of ms. According to the steady state IV curve for fast inactivation, about 50% of the channels are inactivated at -60 mV, and the channels are fully inactivated by -20mV (Rojas et al., 1999) (See fig1-3). In

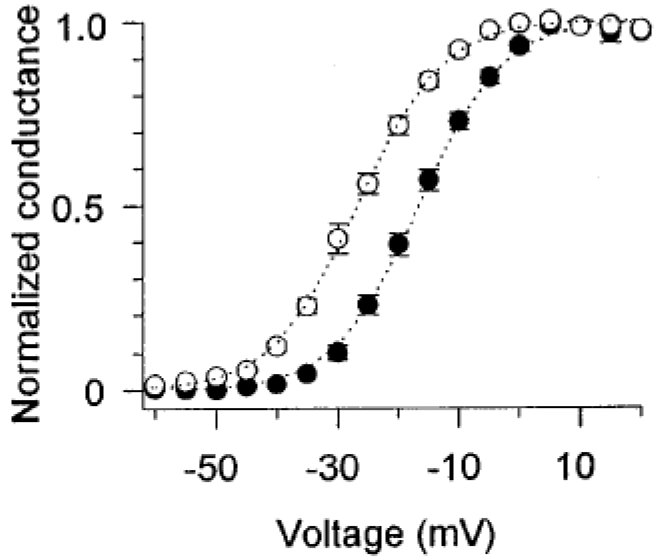


**Figure 1-2. Steady state activation curve of the $Na_V1.4$ channel**. Using voltage clamping techniques, the activation of WT and HyperKPP mutant $Na_V1.4$ was studied. A series of depolarizing pulses were delivered, from a holding potential of -90 mV up to the voltages listed on the X- axis. ● WT ○ M1592V mutant (Figure from Rojas et al., 1999)

addition to providing a method to repolarise the cell membrane, fast inactivation also prevents the AP from travelling in reverse along the membrane by creating a refractory period when additional APs cannot be generated.

There is an additional inactivation process at work in $Na_V1.4$ channels. Slow inactivation occurs over seconds to minutes, and is believed to be important in regulating the number of available $Na_V1.4$ channels in the sarcolemma. Slow inactivation is dependent on the membrane potential, and can be dependent on the history of action potential generation in a fiber (Ruff, 2008, Ulbricht, 2005, Mickus et al., 1999). Experimentally, is has been shown that at no point are 100% of the $Na_V1.4$ channels slow inactivated, even following very long depolarisations. Therefore, there is always a very small fraction of channels available for activation(Featherstone et al., 1996). The entry and exit kinetics of slow inactivation are highly voltage dependent (Vilin and Ruben, 2001, Toib et al., 1998, Vilin et al., 2001) (Fig 1-4). Once again, approximately 50% of the channels can be expected to be inactivated at -60mV (Cummins and Sigworth, 1996). Once $Na_V1.4$ channels begin to be deactivated, there will be a decrease in the amplitude of the $Na^+$ current during subsequent APs. Finally, deactivation is simply the closing of the $Na_V$ channel, and this occurs when the voltage sensor detects that the membrane potential is no longer at threshold.

*The Structure of the $Na_V1.4$ channel:*

The $Na_V$ channel is comprised of two subunits; the larger alpha subunit, and the beta subunit. There are 10 isoforms of the alpha subunit, each found in specific tissues. (Table 1) Each alpha unit isoform comes from a separate gene. The structure of the $Na_V$ channels has been well characterized. The structure of the various isoforms is well conserved, although there are

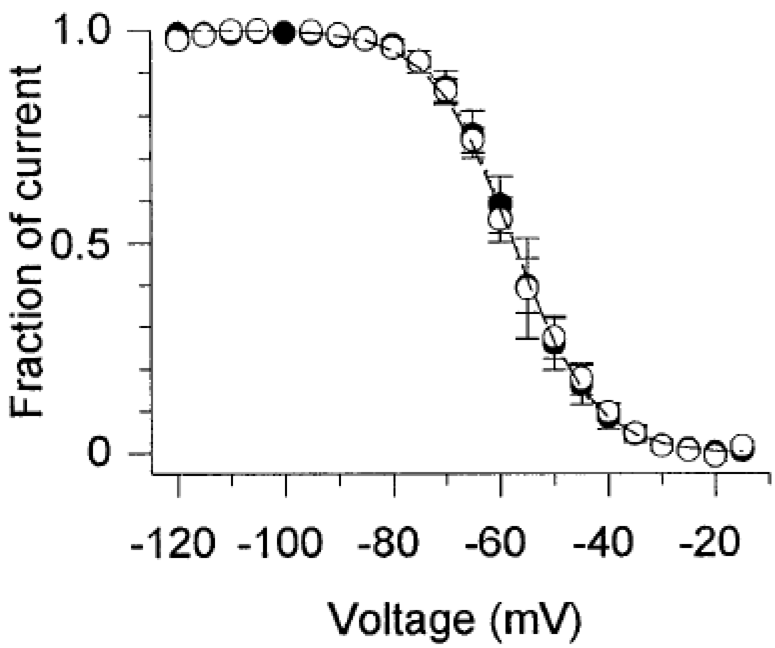


**Figure 1-3. Steady state fast inactivation curves for the $Na_V$1.4.** Holding potential was -140 mV, and a two pulse procedure was used to elicit fast inactivation. 50 msprepulses were administered at the potentials listed on the x axis, followed by a 40 ms test pulse to -10 mV. ● WT ○ M1592V mutant, means plus standard error, n = 14. (Fig from Rojas et al.,1999)

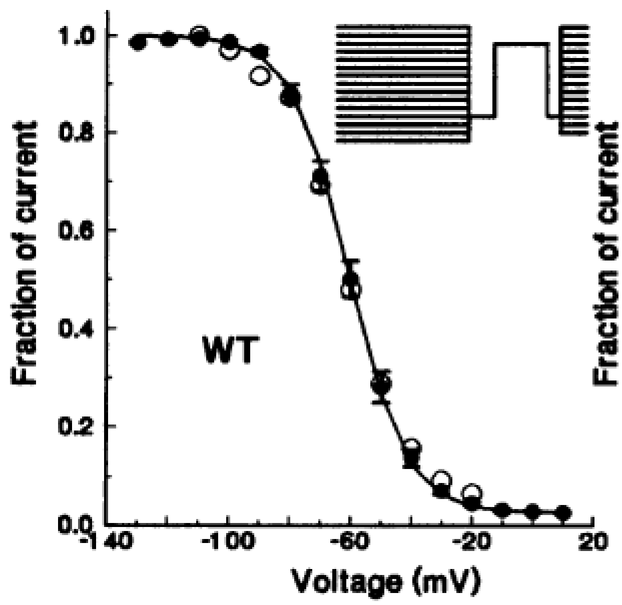


**Figure 1-4. Steady state slow inactivation curve**. Cells were held for 50 s at potentials ranging from -130 mV to +10 mV, in 10 mV increments. Cells were then given a 10 ms recovery pulse to -100 mV, to reverse any fast inactivation. Cells were subsequently given a 20 ms test pulse to -10 mV, and returned to the appropriate holding potential. The current obtained during the test pulse was plotted as a fraction of the maximum current. n=16. Fig from Cummins and Sigworth, 1996

still some key differences observed between isoforms. Some sources indicate that up to 80% of the sequences for each isoform are conserved (Vilin and Ruben, 2001,Fozzard and Hanck, 1996). The $Na_V$1.4 isoform is found in the skeletal muscle, and the $Na_V$ 1.5 isoform is found in cardiac muscle. All other isoforms (NaV1.1-1.3,1.6, 1.9) are found in the neurons(George, 2005,Whitaker et al., 2000).

The structure of the larger alpha subunit consists of four membrane spanning domains (DI – IV) each consisting of six transmembrane segments (SI-SVI)(Duclohier, 2009) (Fig. 1-5). The four domains are homologous, and come together in a ring shape to form the channel (Duclohier, 2009). The S4 segment is highly conserved, and has many basic arginine and lysine amino acids, which under physiological conditions carry a positive charge, and act as the voltage sensor of the channel (George, 2005, Duclohier, 2009, Vicart et al., 2005).Neutralization of these positive charges by amino acid substitutions and manipulation of the channel have definitively shown this area to be the voltage sensor of the channel, since the voltage dependency of the activation curves has been shown to be shifted towards depolarization when this is done(Stuhmer et al., 1997, Groome et al., 2000). All 6 transmembrane segments come together to form the pore structure. Between segments V and VI, there is an extracellular loop of amino acids known as the P loop. These loops come together to form the selectivity barrier for $Na^+$. The study of mutations in the region of segments V and VI have confirmed their role in ion selectivity and permeation (Sato et al., 1998,Guy and Durell, 1994).The intracellular loop between domains III and IV is critical for fast inactivation. The inactivation gate found in this area (Fig.1-5) undergoes a conformational change to block the passage of ions through the channel when the channel is fast inactivated(Vicart et al., 2005, Armstrong and Bezanilla, 1997).The cytoplasmic domain at the C terminus of the protein is also involved with fast

| PROTEIN NAME | GENE | EXPRESSION PROFILE |
| --- | --- | --- |
| $Na_{v1.1}$ | *SCN1A* | Central neurons, peripheral neurons, cardiac myocytes |
| $Na_{v1.2}$ | *SCN2A* | Central neurons, peripheral neurons |
| $Na_{v1.3}$ | *SCN3A* | Central neurons, peripheral neurons, cardiac myocytes |
| $Na_{v1.4}$ | *SCN4A* | Skeletal muscle |
| $Na_{v1.5}$ | *SCN5A* | Cardiac myocytes, uninnervated skeletal muscle, central neurons, fetal myocytes |
| $Na_{v1.6}$ | *SCN8A* | Central neurons, dorsal root ganglia, peripheral neurons, heart, glia cells |
| $Na_{v1.7}$ | *SCN9A* | Dorsal root ganglia, sympathetic neurons, |
| $Na_{v1.8}$ | *SCN10A* | Dorsal root ganglia |
| $Na_{v1.9}$ | *SCN11A* | Dorsal root ganglia |
| $Na_{vx}$ | *SCN7A* | Heart, uterus, skeletal muscle, astrocytes, dorsal root ganglia cells |

**Table 1.1:** List of all of the different isoforms of the alpha subunit of the NaV channel, and their tissue of origin.From Yu and Catterall, 2003.

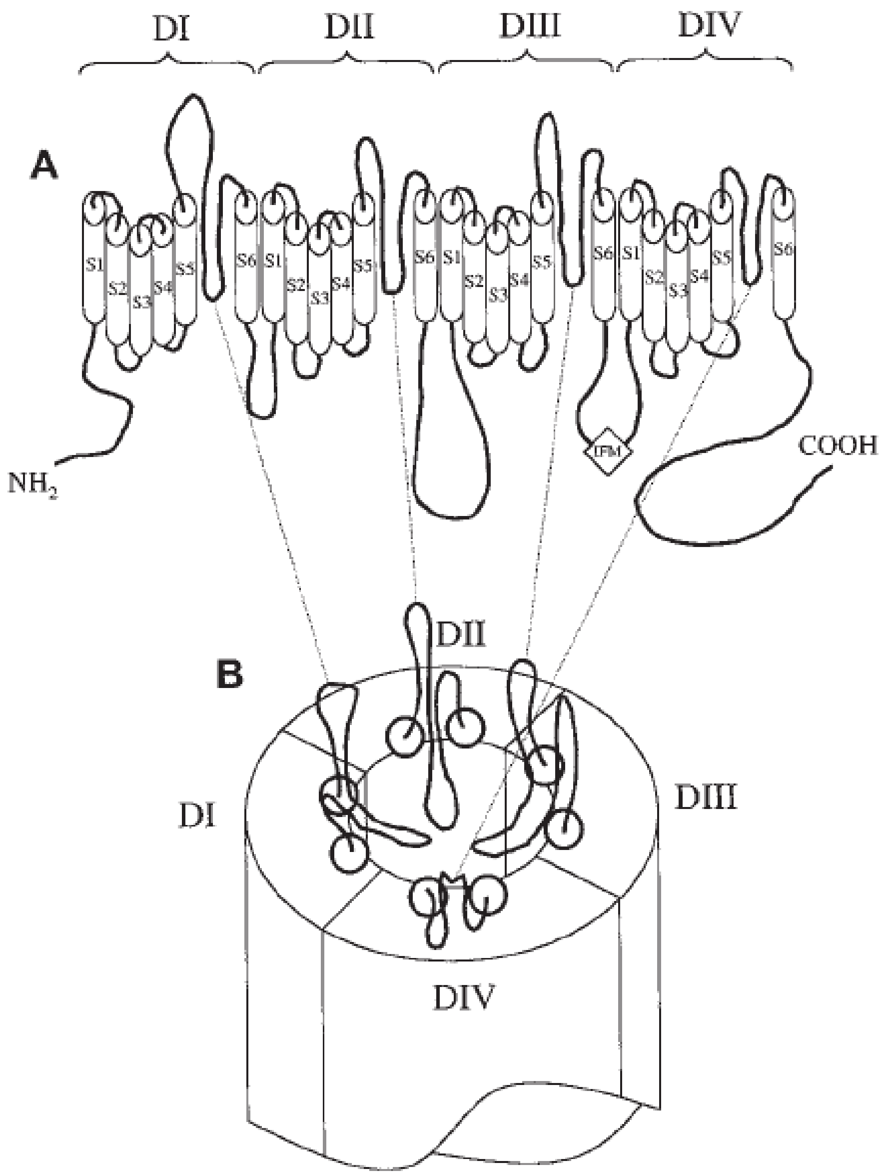


**Figure 1-5: Schematic of the structure of the alpha subunit of the $Na_V$ channel**. A) The 4 domains of 6 transmembrane segments, which are shown as cylinders, shown simplified and unfolded. The inactivation gate is labelled as IFM. B) Schematic of the folded protein showing the P loops. Reproduced from Vilin and Ruben, 2001.

inactivation (Koopman et al., 2006, Motoike et al., 2004). The alpha subunit is thus responsible for the voltage sensory properties of the channel, as well as the formation of the pore, and the ion selectivity.

The beta subunit (33-36kDa) is much smaller than the alpha subunit (230-270kDa)(Rogart et al., 1989, Gellens et al., 1992). Generally, there is one beta subunit associated with one alpha subunit to form the channel, but in some isoforms, there can be two beta subunits associated with one alpha subunit (Isom et al., 1994).$Na_V$ channels in the brain tend to be associated with two beta units, and those in the muscle tend to be associated with only one(Davies et al., 2001, Sugiura et al., 2000). The structure of the beta subunit is much simpler than that of the alpha subunit, consisting only of one transmembrane segment, coupled with a glycosylated extracellular domain, and an intracellular domain (Koopman et al., 2006, Isom et al., 1996). One report suggests that the structure of the extracellular domain resembles that of cell adhesion molecules (Isom et al,1996). The functions of the beta subunits include regulation of the level of expression of the alpha subunit present at the cell membrane, assisting with the control of gating of the channel, as well as some cell adhesion properties, such as attachment to cytoskeletal elements as well as the extracellular matrix (Goldin, 1993, Isom, 2001).

### 1.3 - CHANNELOPATHIES:

A very large number of mutations are known to exist in ion channels within the human body. In the event that the mutation alters the function of the channel, a channelopathy may result. A channelopathy is simply a disease caused by a mutation in an ion channel leading to malfunction of an ion channel, or altered function of the channel. When these channelopathies occur in skeletal muscle, various electrical disturbances can occur, including the two extremes in excitability: myotonia and paralysis. Myotonia involves excessive excitability due to uncontrolled membrane depolarizations leading to uncontrolled activation of the contractile components of the muscle. This in turn leads to a reduction of the muscle`s ability to relax. Mutations in the ClC-1 channel can lead to myotonia congenita, a disorder in which the membrane becomes partially depolarized, causing hyperexcitability (Fig 1-6). Mutations in the $Na_V1.4$ can lead to potassium aggravated myotonia (PAM) another condition where patients experience severe myotonia, caused by a defect in fast inactivation (Lehmann – Horn and Jurkat – Rott, 1999). At the other extreme of symptoms is paralysis. Paralysis arises from a complete lack of membrane excitability within the muscle fibers. Mutations in either the voltage sensitive calcium channel ($Ca_V1.1$) or the $Na_V1.4$ channel can lead to hypokalemic periodic paralysis, a disorder in which paralysis is intermittent. The disorder is named for the very low serum [$K^+$] experienced by patients during paralytic attacks (Lehmann – Horn and Jurkat – Rott, 1999). In addition, some mutations cause both paralysis and myotonia. Mutations in the $Na_V1.4$ disrupting fast inactivation can cause Paramyotonia Congenita, which causes symptoms of both myotonia and paralysis, and is aggravated by the cold (Lehmann – Horn and Jurkat – Rott, 1999). In addition, there are several mutations of the $Na_V1.4$ that are known to Hyperkalemic Periodic Paralysis (HyperKPP), which is the topic of this study.

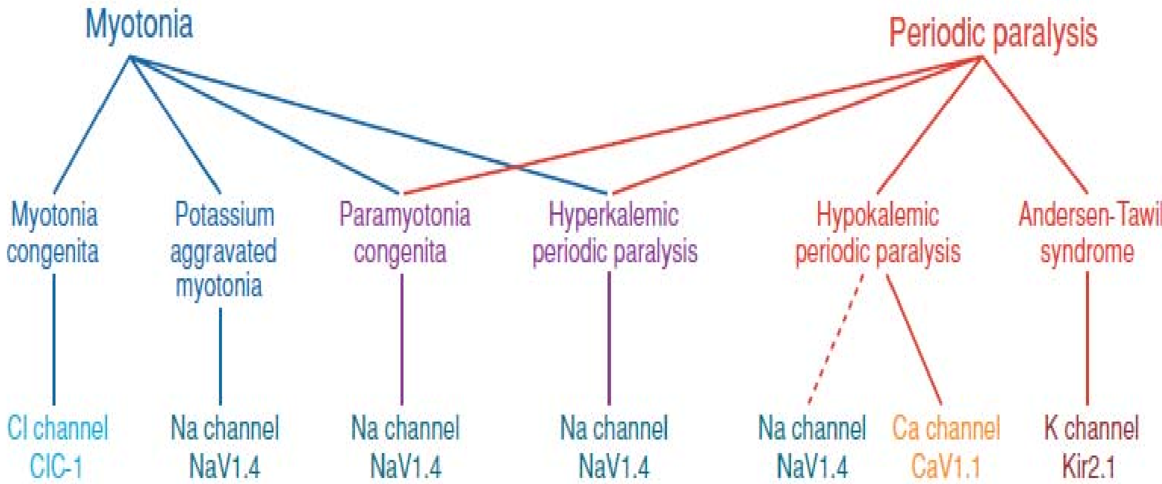


**Fig 1-6. Spectrum of channelopathies in skeletal muscle.** Myotonic disorders on the left, paralysis disorders on the right, and those with both myotonia and paralysis in the center. The channel in which the mutation exists is listed below each disorder name.*Cannon, 2006*

## 1.4 - HYPERKALEMIC PERIODIC PARALYSIS:

Hyperkalemic Periodic Paralysis (HyperKPP) is an inherited muscle disorder characterized by episodes of paralysis and myotonia. HyperKPP is caused by a defect in the skeletal muscle voltage gated sodium channel, $Na_V1.4$ (Fontaine et al., 1990, Miller et al., 2004). Hyperkalemic periodic paralysis is aptly named as the serum $K^+$ level is observed to increase during the episodes of paralysis, sometimes as high as twice the normal values. In patients with HyperKPP, there are three notable defects in the $Na_V1.4$ channel. These defects include: Impaired slow inactivation, impaired activation, and a direct $K^+$ effect causing a non-inactivating mode (Cannon et al., 1991).

HyperKPP is caused by a mutation that is inherited in an autosomal dominant fashion. The mutation has a very high penetrance, which means that those individuals who carry the mutation are very likely to exhibit the phenotype associated with that gene, in this case, the symptoms associated with HyperKPP (Jurkat – Rott and Lehmann –Horn, 2007). HyperKPP is caused by one of nine mutations on the SCN4A gene that codes for the $Na_V1.4$ channel expressed in the skeletal muscle (Jurkat – Rott and Lehmann –Horn, 2007) (Fig. 1-7). Of the 9 mutations, the two most common mutations, T704M and M1592V represent 33% of all cases each, with the remaining 7 mutations causing the remaining 33% of HyperKPP cases. The two most common mutations associated with HyperKPP are point mutations, M1592V (valine replaces methionine at residue 1592) and T704M (methionine replaces threonine at residue 704)(Miller et al.,2004).

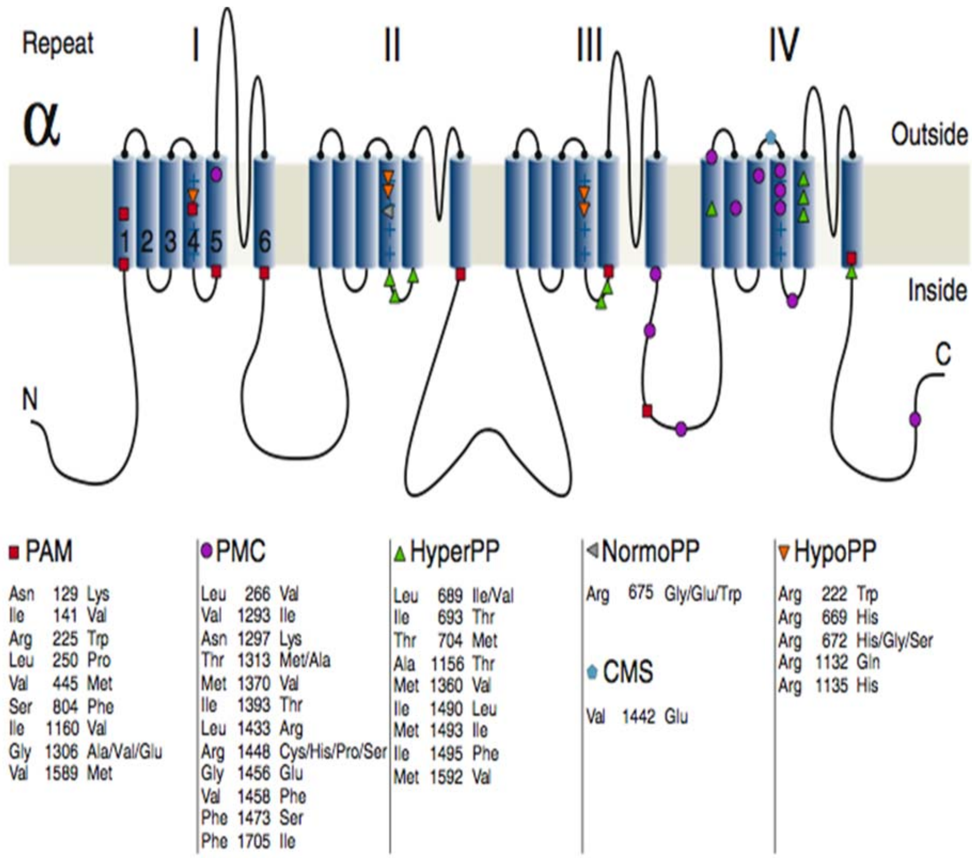


**Figure 1-7. Locations of HyperKPP causing mutations in the $Na_V$ channel.** Schematic shows simplified unfolded $Na_V$ protein with the relative locations of mutations causing 5 different channelopathies. Mutations causing HyperKPP are shown with the green triangles. Jurkatt – Rott et al., 2007

*Symptoms of HyperKPP*

A diagnosis of HyperKPP is based on several clinical observations, as well as genetic markers. Persons afflicted with HyperKPP experience intermittent bouts of paralysis and muscle weakness. Most often, patients experience myotonic discharges, and while they are detectable with an EMG, patients do not always report intrinsic muscle stiffness (Bradley et al., 1990, Jurkat – Rott and Lehmann –Horn, 2007, Lehmann – Horn et al., 2007). This differs from other disorders causing myotonia, where the chief complaint made by patients is of intense muscle stiffness. Most often, HyperKPP presents itself very early in life, with an onset as early as in the first 6 months of life. Approximately half of all HyperKPP affected individuals have their first paralytic attack prior to their 5$^{th}$ birthday, with the vast majority of patients experiencing a paralytic attack in their first decade of life (Gamstrop et al., 1957, Jurkat – Rott and Lehmann – Horn, 2007). As the patients age, the attacks tend to increase in severity and duration, especially following puberty. Once middle age is reached, the paralytic attacks tend to decrease in frequency and in some cases cease completely (Bradley et al., 1990, Gamstrop et al., 1957, Lehmann – Horn et al., 2007, Pearson, 1964). However, some patients report that at this time they experience permanent muscle weakness that precludes their ability to perform some physical tasks, and in a few cases has resulted in dependence on mobility devices such as wheelchairs (Lindinger and Heigenhauser, 1988, Miller et al., 2004, Fontaine, 2008). Generally, the paralysis predominantly affects the limb muscles, and the respiratory muscles of the affected individual remain functional during the paralytic attack, despite the diaphragm containing the mutated $Na_V1.4$ channel. There have however, been some cases in which the patient requires ventilatory support during an attack (Jurkat – Rott and Lehmann –Horn, 2007, Fontaine, 2008).

The presentation of the disease is variable depending on which mutation the patient carries. For example, those with the T704M mutation tend to experience their first attack earlier in life, within their first year, compared to patients with the M1592V who typically experience their first attacks between the ages of 5 and 10. In addition, the frequency of attack is much greater in patients with the T704 mutation compared to those with the M1592V mutation. The average length of paralysis however, is longer in the M1592V mutation. Regardless of the mutation, there is a large degree of variability in the severity and frequency of the paralytic attacks between patients, and in some cases between individual attacks in single patients. Duration of the paralytic attacks is highly variable, with cases reported of paralysis lasting anywhere from a few minutes to several hours, and in a few cases multiple days. Similarly, the frequency of paralytic attacks is variable and the frequency of the attacks can be anywhere from once a month to once or multiple times per day (Miller et al., 2004, Fontaine et al., 2008).

In some cases, patients are able to sense an oncoming bout of paralysis through sensations reported in one case as “creeping heaviness” in the legs (Bradley et al., 1990). Triggers that elicit a paralytic attack are largely patient dependent, however there are some commonalities. Ingestion of $K^+$ salts precipitates an attack in all patients with HyperKPP, as these patients have increased sensitivity to increased $[K^+]_e$. Another very common trigger reported is a period of rest following exercise. Serum $[K^+]$ tends to increase during exercise. The more intense the exercise, the more likely the attack will be severe (Gamstrop et al., 1957, Jurkat – Rott and Lehmann –Horn, 2007, Miller et al.,2004, Fontaine, 2008). Other reported triggers of the paralytic episodes include cold exposure, fasting (which can also lead to an increase in serum $[K^+]$), and emotional stress (Bradley et al., 1990, Gamstrop et al., 1957, Jurkat – Rott and Lehmann –Horn, 2007, Lehmann –Horn, 2007, Miller et al., 2004, Streeten et al., 1971).

Biopsies performed on muscles from afflicted patients have shown several abnormal results, including an increase in type IIA fibers, as well as evidence of fiber damage such as fiber splitting and increased vacuole formation (Gamstrop et al., 1957, Lehmann –Horn, 2007, Miller et al.,2004, Streeten et al., 1971, Fontaine, 2008).

*Electrophysiological Defects*

The predominant defect in HyperKPP is in the slow inactivation. Slow inactivation is responsible for the regulation of the number of excitable $Na_V1.4$ channels as a function of the membrane potential. In HyperKPP, the steady state slow inactivation curve is shifted towards less negative potentials (Fig 1-8).This impaired functioning of slow inactivation causes an increase in the number of $Na_V1.4$ channels that are available for activation compared to WT $Na_V1.4$ channels under the same conditions. For example, at -60 mV, 50% of the WT channels would be slow inactivated, whereas in the T704M mutation only 20% of the channels would be inactivated (Hayward et al., 1997). In addition to the deficit in slow inactivation described above, some of the mutations causing HyperKPP are known to affect activation as well as slow inactivation. (Fig 1-3) Rojas et al. (1997) clearly demonstrate a shift towards hyperpolarization by 5 to 10 mV in the steady state activation curve in cells expressing M1592V mutations. The hyperpolarizing shift in the activation curve coupled with the shift towards less negative potentials in the slow inactivation curve simultaneously create a state in which there is more $Na^+$ current in HyperKPP $Na_V1.4$ channels than in WT channels (Cummins et al., 1993). This persistent additional $Na^+$ current means that there is a larger probability of the mutant $Na_V1.4$ channels being open. In addition to the two defects described above, HyperKPP $Na_V1.4$ channels are particularly sensitive to elevated $[K^+]$. These channels can enter a persistent state of non – inactivation when

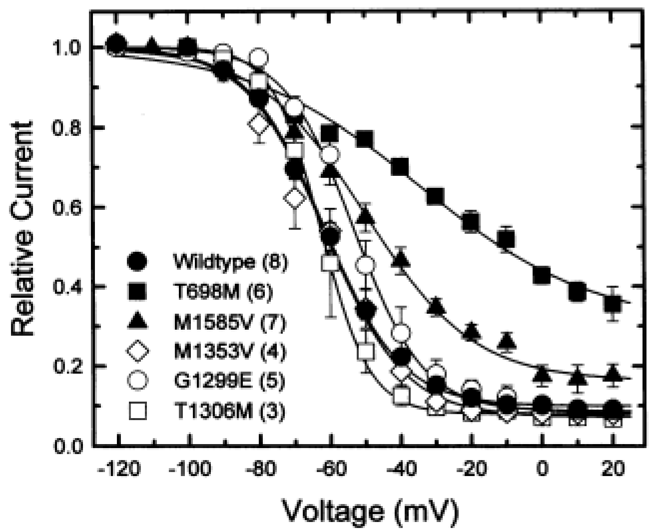


**Figure 1-8. Steady state voltage dependence of slow inactivation.** Cells were held at -100 mV, with a 60 s conditioning pulse. A 20 ms recovery pulse to -100 mV was given to allow channels recovery from fast inactivation followed by a test pulse at -10 mV. Peak current was normalized to the current elicited at the holding potential. From Hayward et al., 1997

exposed to elevated $K^+$. The abnormal non inactivating gating mode is characterized by channels that continuously reopen, and remain in the open state longer than is normal (Cannon, 1991). All of these defects combined lead to abnormal depolarization of the membrane in HyperKPP muscles.

The abnormal depolarization leads to the generation of excess APs not triggered by the motor neurons. These APs are the myotonic discharges (Cannon et al., 1993). Excessive AP generation causes an increase in $[K^+]_e$ due to the efflux of $K^+$ during the repolarization phase. Small increases in $[K^+]_e$ cause slight depolarization of the cell membrane. This depolarization begins a cycle in which the $Na_V1.4$ channels open further, and the mutated channels enter the non – inactivating mode. This leads to a persistent inward $Na^+$ current, further depolarizing the membrane, resulting in even more $K^+$ efflux, more AP generation, and more depolarization. All of this causes the non – mutant $Na_V1.4$ channels to become inactivated, which leads to a loss of membrane excitability and paralysis (Cannon et al., 1991, Lehman – Horn and Jurkat – Rott, 1999) (Fig 1-9).

*Treatment Options*

There are a few treatment and management options available for persons afflicted with HyperKPP. Avoidance of food that contains large amounts of $K^+$ is an easy way to avoid triggering attacks through consumption of potassium (Jurkat – Rott and Lehmann –Horn, 2007). Mild exercise has been shown to be effective in helping to avoid the paralytic attacks (Bradley et al., 1990, Gamstrop et al., 1957, Jurkat – Rott and Lehmann –Horn, 2007, Lehmann-Horn 2007).

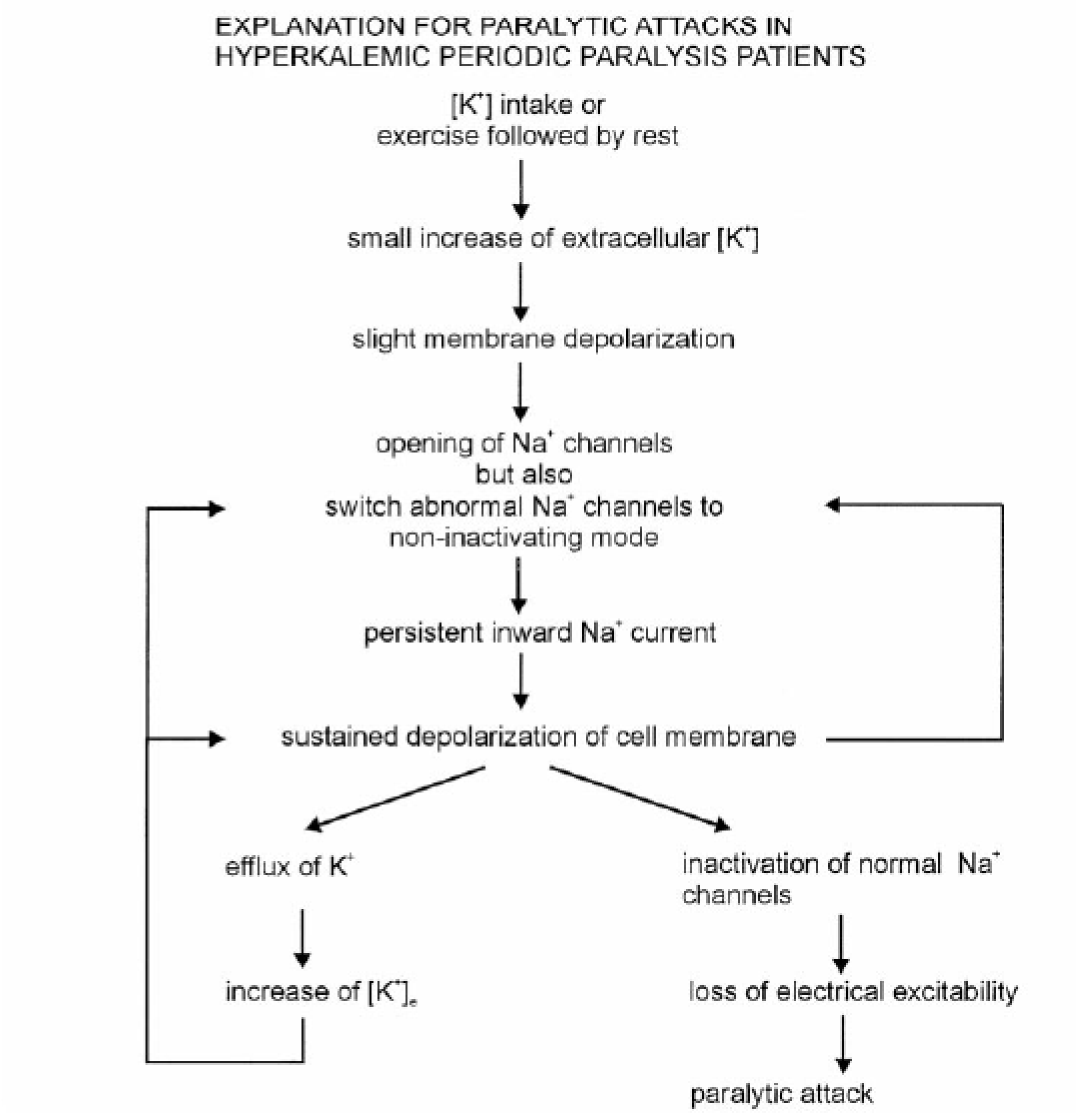


**Figure 1-9. Cycle leading to paralysis in HyperKPP muscles.** Flow chart representation of the presumed sequence of events in HyperKPP muscles giving rise to paralysis. From Lehmann Horn and Jurkat – Rott, 1999

Select cases have shown that the ingestion of glucose or simple intake of foods not containing $K^+$ can shorten the paralytic episode (Gamstrop et al., 1957). The pharmacological interventions for patients suffering HyperKPP include acetazolamide, a carbonic anhydrase inhibitor, and the $Na^+$ - $K^+$ pump activator salbutamol. However, acetazolamide simply reduces the frequency of the attacks, not the duration, and in some cases ceases to be helpful (Bradley et al., 1990, Lehmann-Horn 2007, Pearson, 1964, Streeten et al., 1971). Salbutamol appears promising as a treatment option, as it is quite effective over the short term, however, it quickly becomes ineffective (Clausen et al., 1980, Wang et al., 1976).Some cases have shown that calcium gluconate can reduce the severity of the paralytic attacks (Gamstrop et al., 1957, Pearson, 1964). There are no fully effective treatments for HyperKPP currently in existence.

The mechanism through which $Ca^{2+}$ is benefitting patients is currently unknown. Being the subject of this thesis, the next section will discuss how $Ca^{2+}$affects membrane excitability and contraction in normal muscles.

## 1.5 THE ROLE AND IMPACT OF $Ca^{2+}$ IN MUSCLE CELLS:

As discussed above, $Ca^{2+}$plays an important in the activation of the contractile components, acting as the messenger between action potential in the cell membrane to the final activation of contractile components in the sarcomere. In addition, $Ca^{2+}$ has an important role in regulation and signalling within the muscle fibers. $Ca^{2+}$ ions are heavily involved in muscle plasticity, especially with regard to modulation of fiber types. Conditions of increased stimulation cause a chronic increase in intracellular $Ca^{2+}$. This can then activate the mediator calcineurin, a calcium dependant phosphatase, which acts as a mediator of fiber type changes in the muscles. It has been shown that in fibers heavily expressing calcineurin, there is an increased likelihood of observing slow type fibers (Berchtold et al., 2000).

The effects of $Ca^{2+}$ are not limited to the activation of the contractile components. It has also been shown that prolonged electrical stimulation leads to accumulation of $Ca^{2+}$ ions in the sarcoplasm, an effect which is at least partially mediated by the $Na_V1.4$ (Gissel and Clausen, 1999). Increased concentrations of $Ca^{2+}$ ions are known to cause a shift in the voltage dependence of activation of $Na_V$. For example, when $[Ca^{2+}]$ is raised to 40 mM, this curve is shifted 30 mV towards less negative potentials (Hanin and Campbell, 1983).This leads to a membrane that is more easily excited. This same increased $[Ca^{2+}]$ also shifts the inactivation curve towards less negative potentials, which would cause the $Na_V$ channels to become inactivated later than anticipated (Hanin and Campbell, 1983).Furthermore, increased $[Ca^{2+}]$ has an effect on the gating current. The current voltage relationship was also shifted towards less negative potentials (Hanin and Campbell, 1983). While these experiments illustrate the effect of $Ca^{2+}$ on the $Na_V$ channel dramatically, 40 mM is not a physiologically relevant concentration of $Ca^{2+}$.

When $[Ca^{2+}]$ becomes depleted, there is a detrimental effect leading to pronounced fatigue (Cairns et al., 1998). This may be an indication that force depression due to fatigue may be in fact due to t -tubular $Ca^{2+}$ depletion (Cairns et al., 1998). Increased concentrations of 10 mM $Ca^{2+}$ have a positive effect in fatigued muscle with elevated $K^+$ of 10-12 mM. It is postulated that the restoration of force obtained in such muscles by adding 10 mM $Ca^{2+}$ is due to a ~ 5 mV reversal of the depolarization caused by the elevated $K^+$ (Cairns et al., 1998). This observation of increased force production in $K^+$ depressed muscles treated with elevated $Ca^{2+}$ provides a partial basis for the beneficial effects of $Ca^{2+}$ in patients with HyperKPP. Finally, it has been well established that divalent cations have a 'shielding' effect on membranes, which tends to reduce the current through the $Na^+$ channel (Gissel and Clausen, 1991). This too could explain some of the benefit seen in patients with HyperKPP given that the primary defect in this disease is an excess of $Na^+$ influx into the cell.

Large conductance, voltage and calcium gated potassium channels (BK Channels) are present in neurons, smooth muscle and skeletal muscle. These channels are activated by membrane depolarization, and also by increases in $[Ca^{2+}]_i$. In smooth muscle cells, the BK channel is important for the development of muscular tone. In neurons, the BK channel plays an important role in the repolarization and hyperpolarization during an action potential generation, and the same may be true in skeletal muscle. However, the function of the BK channel in skeletal muscle is currently unknown. The BK channel presents a potential mechanism through which $Ca^{2+}$ may be benefitting patients with HyperKPP since its function in other tissues is to hyperpolarize the membrane, which would be very useful in patients with HyperKPP that experience chronic depolarization.

Even though $Ca^{2+}$ treatments are not completely effective in HyperKPP patients, it is important to understand the mechanism through which these treatments are acting. If the mechanism through which $Ca^{2+}$ is benefitting patients is understood, we will have gained a better knowledge of the disease itself, and developed a target pathway for novel treatments. Even though $Ca^{2+}$ cannot be used in the long term as treatment for these patients, it is possible the mechanism through which it acts will be able to be exploited by pharmaceuticals or other targeted treatments.

## 1.6 HYPOTHESIS AND OBJECTIVES:

The overall hypothesis of this study is "that $Ca^{2+}$ alleviates HyperKPP symptoms by i)activating the BK channel leading to membrane repolarisation and ii)by directly reducing $Na^{+}$ influx through its channels".

To start addressing the question as to whether BK channels are involved, the first aim will be to measure that increased in $[Ca^{2+}]_e$ results in increases in $[Ca^{2+}]_i$. The second aim will be to determine that the increase in $[Ca^{2+}]_i$ is large enough to activate BK channels in HyperKPP muscles. To further test that an activation of BK channels is responsible for the alleviation of symptoms, aim 3 will be to determine if blocking BK channels prevent the beneficiary effects of $Ca^{2+}$. Finally, to determine if the partial effect of $Ca^{2+}$is due to an insufficient activation of BK channels, aim 4 will be to test whether a pharmacological activation of BK channels better improve the functionality of HyperKPP muscles than an increase in $[Ca^{2+}]_e$.To test whether $Ca^{2+}$alleviates the severity of the paralytic attacks by impacting the $Na^{+}$ influx itself, the fifth aim will be to document how an increased in $[Ca^{2+}]_e$ affects $Na^{+}$ influx in HyperKPP muscles.

Finally, a sixth aim was added in which the myotonic discharge was measured in live HyperKPP mice. These measurements were important to eventually be able to test any potential pharmacological approach to treat HyperKPP symptoms. These measurements were part of an aging study undertaken by the laboratory to better understand the progression of the disease n mice

# CHAPTER 2: MATERIALS AND METHODS

Animals:

The generation of HyperKPP mice was completed by knocking in the human equivalent missense mutation M1592V into the genome of FVB1N background mice. In mice, this mutation is a methionine to valine at position 1585 (Hayward et al., 2008). Mice used for experiments were heterozygous, as the homozygous mutants do not survive past birth(Hayward et al., 2008). Heterozygous HyperKPP mice were continually bred with FVB1N background mice to establish a colony. FVB1N mice were used as a wild type for all experiments except for single fiber experiments where CD1 animals were used instead. All mice were fed *ad libitum* and housed according to the guidelines of the Canadian Council for Animal Care. The Animal Care Committee of the University of Ottawa approved all experimental procedures used in this study. Prior to muscle dissection, mice were anaesthetized with a single intraperitoneal injection of 2.2 mg ketamine/0.4 mg xylazine /0.22 mg acepromazine per 10 g of animal body weight, followed by cervical dislocation. Experiments involved the use of intact Extensor digitorum longus (EDL), and soleus muscles, Flexor digitalis brevum (FDB) bundles and single fibers.

Genotyping:

Mice were genotyped using a section of the tail that was clipped at the time of weaning. A 2 mm tail piece was incubated overnight with 500 µL tail digestion buffer (0.2 mM disodium EDTA and 25 mMNaOH, pH 12.3) and 50 µL Proteinase K (1mg/mL) at 56 °C. DNA extraction was completed following the overnight incubation. 650 µL of 1:1 Phenol:CIA was added to each tube, and centrifuged 10 min at 12000 g. (Heraeus instruments, Biofuge 15**)** The top layer was removed to a new tube, to which 650 µL of CIA was then added and centrifugation was repeated. This step was repeated twice. The top phase was again removed to a fresh tube, and 750 µL of isopropyl alcohol was added. Solutions were allowed to rest 10 min at room temperature, followed by centrifugation for 15 min at 15000 g. All of the alcohol was removed following centrifugation, and 750 µL of 70% ethanol was added to the pellet, and centrifugation repeated. Once again, all alcohol was removed to allow the pellet to air dry for 30 min prior to resuspension with 200 µL of TE buffer (10mM Tris, 1 mM EDTA, pH 8.0) and incubated at 65°C for 2 hours. Polymerase chain reaction (PCR) was run using the following primers:

NC1F (forward): 5' TGT CTA ACT TCG CCT ACG TCA A 3'

NC2R (reverse): 5' GAG TCA CCC AGT ACC TCT TTG G 3'

The PCR product was digested 2 – 6 hrs using the restriction digest enzyme NSP1 temperature. The mutation that is knocked in to the HyperKPP mice genome causes the removal of the NSP1 splice site. Therefore, when the digest product is run on an electrophoresis gel, two bands will be visualized for WT animals, which carry the splice site on both alleles and three bands will be seen for HyperKPP animals, which have one normal allele and one mutated allele lackingtheNSP1digestion site.

<u>Single Fiber Preparation:</u>

Single muscle fibers were isolated as per Cifelli*et al.* (2007). Briefly, mouse FDB muscles were incubated3 hrs at 37°C in an MEM culture solution (Gibco) supplemented with 10% fetal bovine serum (FBS, Gibco)containing 0.2% (w/v) type 1collagenase (Sigma). Single fibers were separated by trituration with a plastic pipette while in fresh MEM not containing any collagenase. A small volume (150 µL) of solution containing 50-85 fibers was put onto Matrigel coated glass coverslips and allowed to settle 30 min prior to the addition of 1 ml of MEM. Fibers were kept at 37°C until they were used on the same day. Contractile characteristics of the fibers were determined by placing coverslips in an RC-25 chamber (Warner Instruments, Canada) preheated to 37°C and were superfused with physiological solution at a rate of 2-3 ml per min. Temperature was maintained with a dual channel heater. (model TC-344B, Warner Instruments)

Physiological solution:

Control physiological saline solution contained (in mM): 118.5 NaCl, 4.7 KCl, 1.3 $CaCl_2$, 3.1 $MgCl_2$, 25 $NaHCO_3$, 2 $NaH_2PO_4$ and 5.5 D-Glucose. Solutions containing higher $[K^+]e$, $[Ca^{2+}]e$ or $[Mg^{2+}]e$ were prepared by adding appropriate amounts of KCl, $CaCl_2$ or $MgCl_2$. All solutions were continuously bubbled with 5% $CO_2$/95% $O_2$ gas to maintain pH of 7.4. All experiments were conducted at an experimental temperature of 37 °C.

Force measurements:

Force was measured using small FDB bundles as described by Cifelli. (2007). Briefly, bundles were superfused with physiological solution in a horizontal Plexiglas chamber at a rate of 15 mL/min. Muscle bundles were attached to a force transducer (Model # 400A, Aurora Scientific, Canada) via silk knots on the tendons. One tendon was fixed to a stainless steel wire hooked to the transducer, and the other was attached to stationary hooks. Muscle length was adjusted to provide maximum tetanic force. Force transducers were connected to a KCP13104 data acquisition system (Keithley, USA). Data was acquired and recorded at 5 kHz. Peak tetanic force, unstimulated force and peak total force were analyzed.

Tetanic contractions were elicited using electrical stimulation via two platinum wires located on opposite sides of the muscle bundle. The platinum wires were connected to a Grass

S88 stimulator (Grass technologies) as well as an isolation unit (Grass technologies SIU5). Tetanic contractions were elicited using 200 ms trains of 0.3 ms, 10 V pulses, with a stimulation frequency of 200 Hz. Tetanic contractions were elicited every 100 s.

<u>$Ca^{2+}$ and $Na^{+}$ influx measurements:</u>

EDL and soleus muscles were dissected in physiological solution and then mounted vertically into chambers consisting of methyl acrylate cuvettes. Muscles were incubated in 2 ml physiological solution for a 30 minute equilibrium period. For $Ca^{2+}$ influx experiments, muscles were incubated for 15 min with 1 μCi/mL $^{45}Ca^{2+}$.The extracellular $^{45}Ca^{2+}$ was then removed with four 30 min washouts. For $Na^{+}$ influx, muscles were incubated10 min with 2 μCi/ mL $^{22}Na^{+}$ followed by washout for 5 minutes, 10 minutes, 15 minutes, and 15 minutes, again to remove all extracellular $^{22}Na^{+}$. All washout solutions were comprised of 10 mM HEPES, 280 mM Sucrose, 500 nM TTX, the latter to fully block Nav1.4 channels. Following washouts, muscles were patted dry and weighed. Muscles used for $Na^{+}$ influx were put into plastic scintillation vials and read with a gamma counter (Wallac, 1282 Compugamma). Muscles used in $Ca^{2+}$ influx experiments were put into tubes containing 2 mlof 6% perchloric acid and homogenized. The homogenized muscle solution was centrifuged 5 minat 12000 g and 1.0 mlof supernatant was added to10 mlof Ecolume Scintillation fluid (MP Biosciences). $^{45}Ca^{2+}$ was counted using a β counter (Wallac Instruments, model 1414).

EMG measurements:

Animals were anaesthetized using inhaled 2% isofluroanegas. Two electrodes (S06666-0 and S03355-90H, Rochester electromedical) were then implanted in the gastrocnemius muscle, and one in the mid back to act as a ground, and then incisions were closed. Mice were allowed to recoverfrom the anaesthetic. All mice exhibited normal behaviour upon removal from the anaesthetic, and subsequently the electrodes were attached to an amplifier (Grass technologies, P55 AC Pre amplifier**)** and into the KCPI 3104 data acquisition system. EMG traces were saved at 10 kHz and later analyzed. Throughout the data acquisition period, the animal was continuously observed, and its behaviour noted into the computer. Animal behaviours were classified as either being in the resting position, or being in the active state. Animals who were in the resting position had all 4 limbs on the ground, and were stationary, except for small head movements. Animals that were not in the resting position were considered to be in the active state.

# CHAPTER 3: RESULTS

## 3.1-EMG MEASUREMENTS

The aim of the EMG measurements was to empirically measure the HyperKPP symptoms experienced by affected animals, including paralysis and myotonic discharge. Throughout the experiments, mice were free to move around their cages as they pleased. All of the HyperKPP animals used were reported to have previously experienced paralysis by animal care technicians. These episodes of paralysis consisted of animals being completely paralysed without an escape reflex, or in some cases with animals dragging their hind limbs behind them. In all cases, the paralytic episodes were transient and brief, lasting no more than 1 minute. However, over the course of all of the experiments conducted, no episodes of paralysis were observed in any of the animals tested. Contrary to the lack of paralytic attack, evidence of extra electrical activity (possibly due to myotonic discharge) was obtained. EMG data were separated according to what mice were doing. Mice were designated as being in a resting position if it was in a prone position, resting on all four limbs, calm and unmoving. Mice were classified as active if it was moving, resting on fewer than all four limbs or agitated in any way. Representative EMG traces of mice that were active, resting and under anaesthesia are shown in Fig 3-1. Traces taken when mice were under anaesthesia show complete abolishment of EMG activity. In addition, traces with manual leg movement with the mouse under anaesthesia also show a completely flat curve. This was done to ensure that the entire signal obtained via EMG was due to action potential generation in muscle, and not due to noise or friction caused by movement of the animal. When mice were resting, there is noticeably less electrical activity than when mice

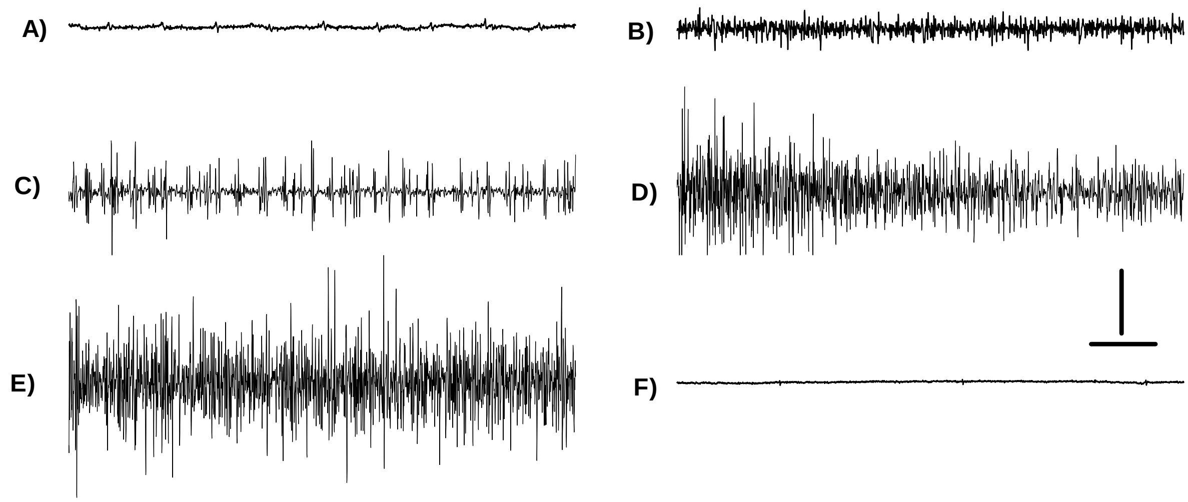


**Figure 3-1.Examples of EMG traces from gastrocnemius muscles.** When mice were in the resting position, a very low level of EMG activity was observed, especially in W.T. mice (A); slight increases in EMG activity either continuously (B) or intermittently (C) were also observed in mice in the resting position. In some cases there was greater EMG activity (D), especially in HyperKPP mice. When mice were in the active state, a high level of EMG activity was observed (E). At the end of each measurement, EMG traces were recorded after mice had been anesthetized and while vigorously moving the leg. For both W.T. and HyperKPP mice, the EMG trace became quiet following anesthesia even when the leg was moved (F). Vertical bar represents 5 µV; horizontal bar represents 100 msec.

were active. The active traces show larger numbers of peaks and higher maximum voltages than their resting counterparts.

In order to determine if there was increased electrical activity in HyperKPP muscles, the most important consideration when looking at the EMG data was the surface area under the curve. This is because the EMG is in effect a summation of action potential in muscle. When there were increased numbers of action potentials, the amplitude of the EMG signal increased, which will in turn cause an increase in the surface area measured under the curve. To analyse the surface area, the original EMG trace was rectified so all voltages were positive (Fig 3-2). The area under the curve was then calculated and added over time. The different slopes of the resulting lines were then calculated to determine the rate of increase in surface area over time. In order to determine a suitable amount of data to be analysed to obtain a representative sample, 10 minutes each of resting position and active data were analysed, and results for 2.5 minutes, 5 minutes, 7.5 minutes and 10 minutes of data were compared. When considering the resting time, it was found that 2.5 minutes was insufficient to be representative, as with only 2.5 minutes of data, the curve was shifted to the right compared to those of 5, 7.5 and 10 minutes of data. (Fig 3-3) However, it was found that 10 minutes of data was sufficiently representative for both active and resting position time, and thus it was determined that henceforth 10 minutes of active time and 10 minutes of rest time would be analysed.

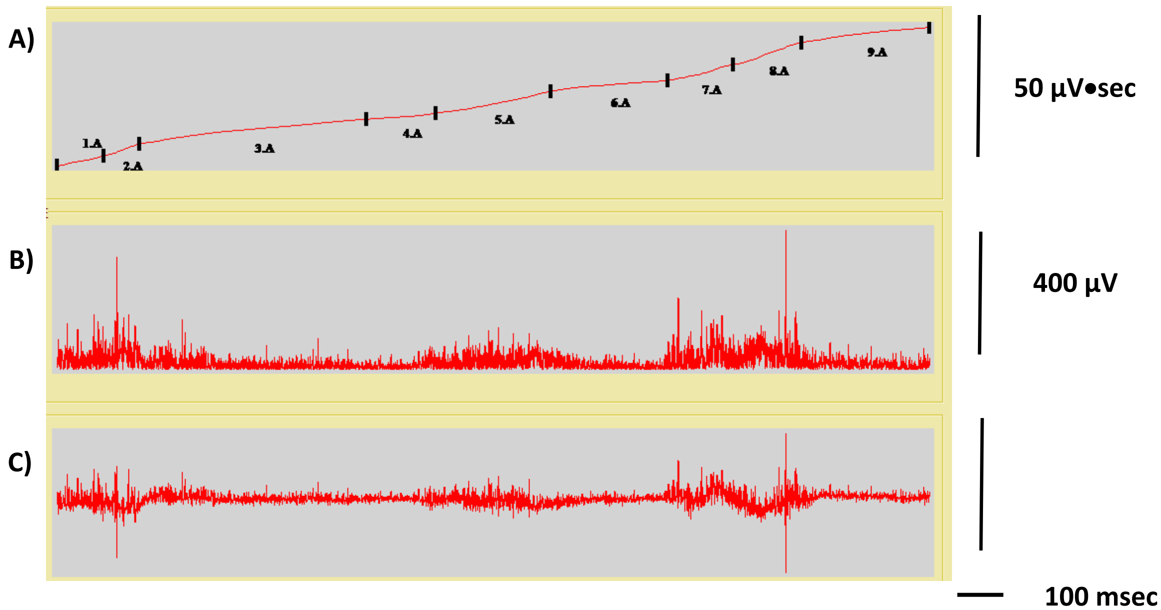


**Figure 3-2. Screen capture of the EMG analysis program**. A two sec segment of an EMG trace (C) which was rectified (B) to calculate the increase in EMG surface area under the curve (A). The rates at which the surface area increases over time were not constant and were divided into segments of constant rates (small vertical bars). The slope of each segment was calculated using a linear regression analysis. Letter A indicates that these EMG signals were obtained while the mouse was active.

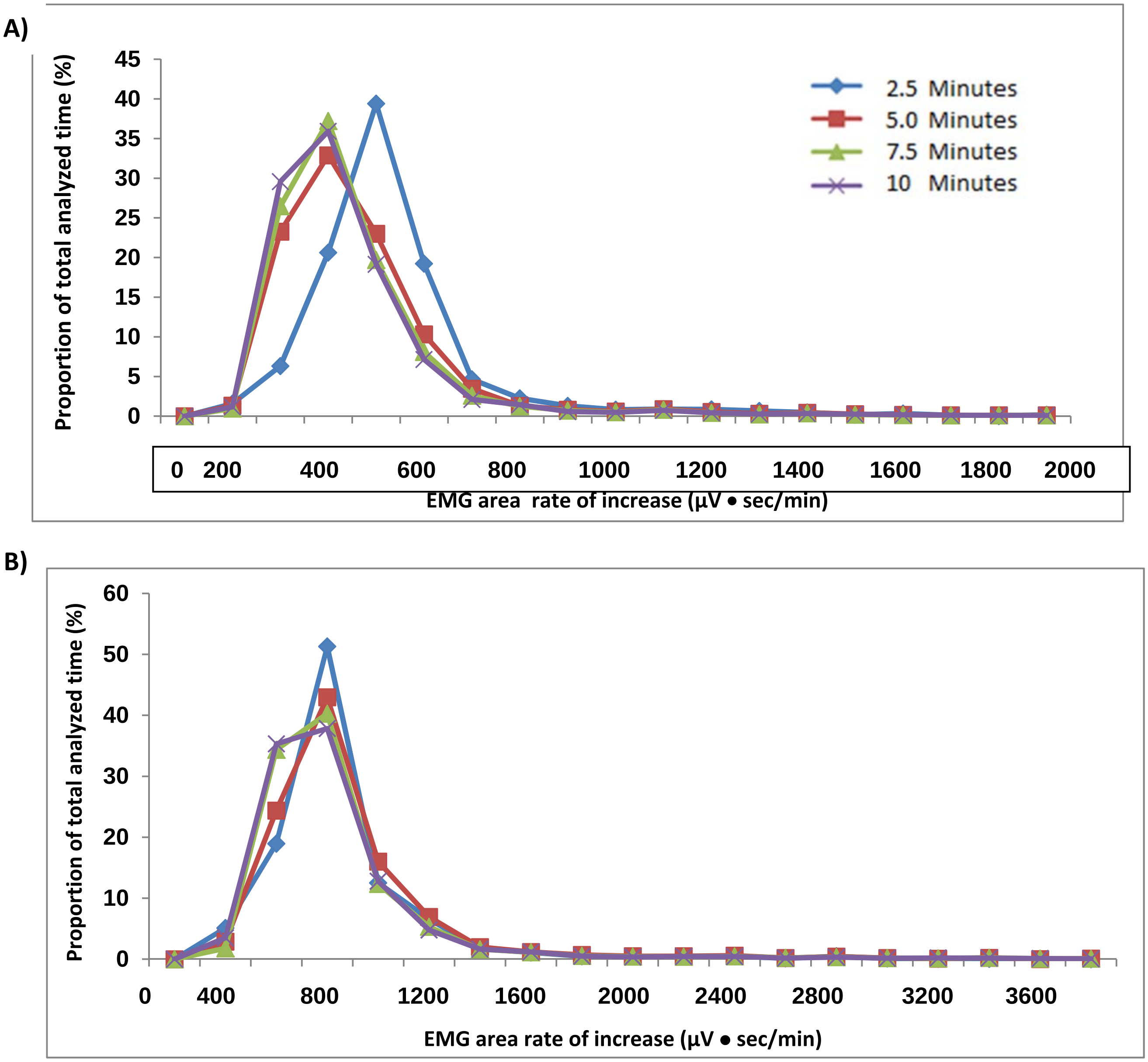


**Figure 3-3. Ten minutes of data is sufficient to analyze for both A) resting and B) active mice.** EMG surface area under the curve was measured as described in text and in figure 3-2. Slopes were divided in ranges of 200 µV*sec / min and the time during which each range was observed was added and then expressed as a percentage of the total time. The first 10 minutes of both resting and active time (20 minutes total) are shown here, in 5 minute increments.

In the 8 week old animals, EMG measurements were taken with 2 protocols. One protocol in which multiple 800 ms sweeps of data were accumulated over several hours, and the other as described above. The results from both protocols were very similar, and the results from the 800 ms sweep protocol can be found in Appendix I. For resting 8 week old WT mice, half of the time the area under the EMG curve increased at a rate between 400 and 600 µV•sec per min. Rates of increase between 600 and 800 µV•sec per min, and between 800 and 1000 µV•sec per min occupied 20% and 10% of the time respectively (Fig 3-4). The rate of increase above 1000 µV•sec per min was less than 5% of the time. For HyperKPP mice, the curve was shifted toward higher rates of increase, with only 20% of the time at a rate between 400 and 600 µV•sec per min vs the 50% value seen in the WT mice.

In 8 week old HyperKPP mice, rates of increase between 600 and 800 µV•sec per min, and 800 to 1000 µV•sec per min were more common than in WT, occurring at frequencies of 25% and 15% respectively. Additionally, where in WT mice nearly 50% of the time the slope was between 400 and 600 µV•sec per min, this only occurred in the HyperKPP mice at a frequency of 22%. Another large difference between WT and HyperKPP mice appears when considering rates of increase above 1000 µV•sec per min, where in HyperKPP mice these values occurred about 40% of the time, compared to only 10% in WT mice. Additionally, in WT mice, values between 0 and 200 µV•sec per min were observed at a frequency of nearly 10%, yet in HyperKPP mice, no values were observed in this range. One final observation is that at rest in HyperKPP animals, there is a noticeable increase in the frequency of values in the range of 2200 µV•sec per min. Although the frequency for this range was not large, (~3%) the increase relative to the WT was observed not only using the continuous acquisition protocol, but also with the preliminary trials using 800 ms traces. (See Appendix 1).

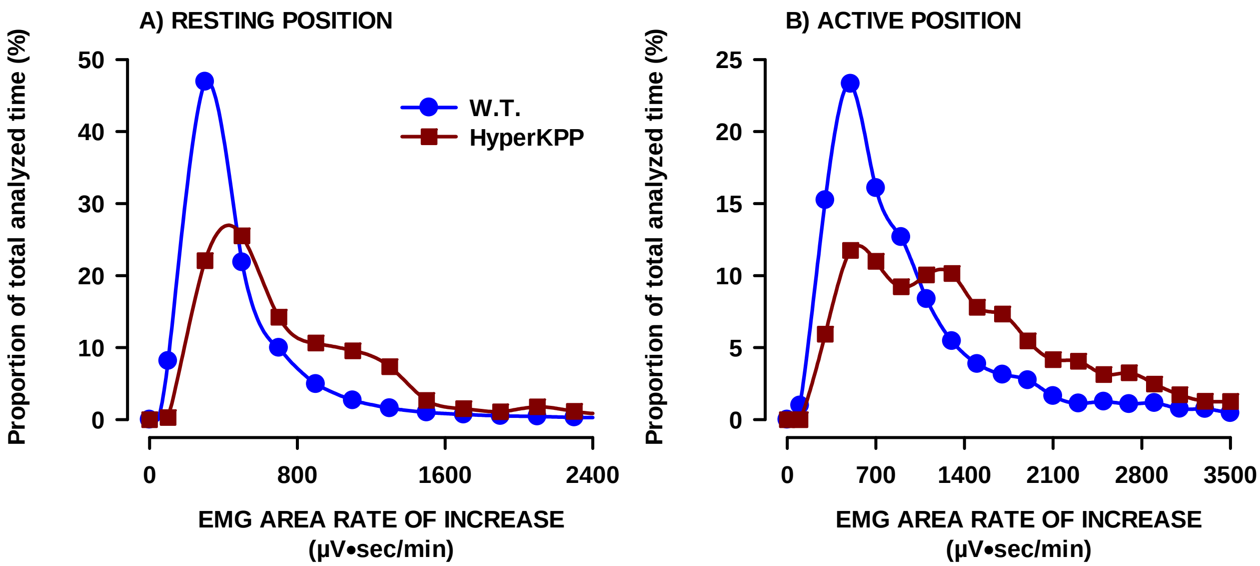


**Figure 3-4. Frequency distribution of the rate of increase of the area under the EMG curve is shifted towards larger values in HyperKPP mice for both A) resting and B) active mice.** Rates of increase were separated into bins of 200 µV•sec/min, calculated as described in the text, and the amount of time for each rate bin was expressed as a % of the total time analyzed. Mice used were 8 weeks old (n=5)

In the WT animals, the peak value for the resting positionwas at 400 µV•sec permin, where the peak for active animalswas found at 600µV•sec per min(Fig.3-4).In general, the frequency distribution for the active state was shifted toward higher rates of increase than in animals in the resting position. In active WT animals, the slope was between 600 and 800 µV•sec per min 25% of the time, and was between 800 and 1000 µV•sec per min 17% of the time. It is to be noted, however, that there is a much greater range of values for mice that are active vs. mice in the resting state. For WT mice in the resting state, there were values greater than 1400 µV•sec per min reported approximately 5% of the time. For WT mice that were active, values greater than 1400 µV•sec per min were more common, accounting for approximately 20% of all values. The shape of the curve obtained from resting WT mice is also different than that of the active mice. In resting mice, there is a pronounced peak (at 400µV•sec per min), followed by a rapid decline to 0 (at ~1400 µV•sec per min). For the active state, there was still a peak, at 600 µV•sec per min, but the decline to 0% frequency was much more gradual, and never completely reaches 0%, with values reported at small frequencies (~1%) all the way to 3600 µV•sec per min.

Just as for the WT, the frequency distribution for HyperKPP mice in the active state was shifted towards higher frequencies. For HyperKPP animals in the active state, the slope was between 600 and 800 µV•sec per min 12% of the time, and was between 800 and 1000 µV•sec per min for only 10% of the time, compared to 25 and 17% of the time for WT. µV•sec per min. Additionally, there is a much higher frequency of slopes greater than 1400 µV•sec per min in active HyperKPP mice, occurring at a frequency of nearly 50%, compared to 20% for active WT mice. Furthermore, the shape of the curve is completely different than any other in the active HyperKPP mice. Where there is a peak followed by a decline for WT resting position, active state, and HyperKPP resting position, there is a plateau and a very steady decline in active

HyperKPP mice, with the curve never fully reaching zero, even at 3600 µV•sec per min. Typical of the presentation of HyperKPP in humans, there is a large amount of variability in the presentation of the disease in the mouse model. This was true for the results of the EMG section, with large variability between HyperKPP animals tested with EMG (See appendix 2). For this reason it was impractical to include standard error on fig. 3-4. In general, there is increased electrical activity observed when the HyperKPP mice are both in the resting position and the active state. As the level of activity increases in the EMG, itis indicative of increased action potential generation.These increases in AP generation are characteristic of the myotonic discharge portion of HyperKPP.

The total area under the rectified EMG curve was also calculated. For WT mice in the resting position, the mean area under the EMG curve was 5,634 µV•sec for a period of 10 minutes, whereas for HyperKPP mice the value was 8,690µV·sec (Fig 3-5). This represented an increase of approximately 50%. For mice in the active state, the difference between WT and HyperKPP animals was even larger, with values of 11,056 µV•sec and 19,234µV•sec for WT and HyperKPP animals respectively, an increase of nearly 75%.In general, the overall electrical activity as measured from the EMG traces was greater in the HyperKPP mice than in WT mice, in both the resting position and active state.

In order to determine the progression of symptoms in HyperKPP mice, EMG experiments were also conducted on mice that were 3, and 24 weeks of age. In the resting position, there was not a large difference between 8 and 24 week old HyperKPP mice, with the slope between 400 and 600 µV•sec per min 22% or 20% of the time, respectively (Fig 3-6).For slope values between 600 and 800 µV•sec per min, frequencies were 25% and 20% for 8 and 24 week old

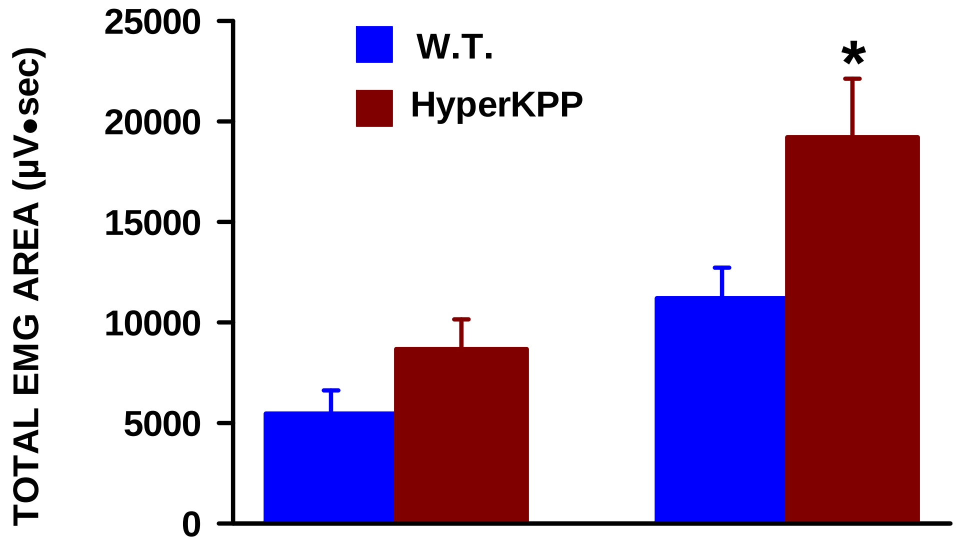


**Figure 3-5. The mean total area under the EMG trace was higher in HyperKPP gastrocnemius muscle than for WT, both for resting (left) and active (right) animals.** The total area was calculated for each mouse and then averaged. Vertical bars represent SE of 5 mice.

***** Significantly different from wild type muscle, ANOVA and L.S.D., $P < 0.05$.

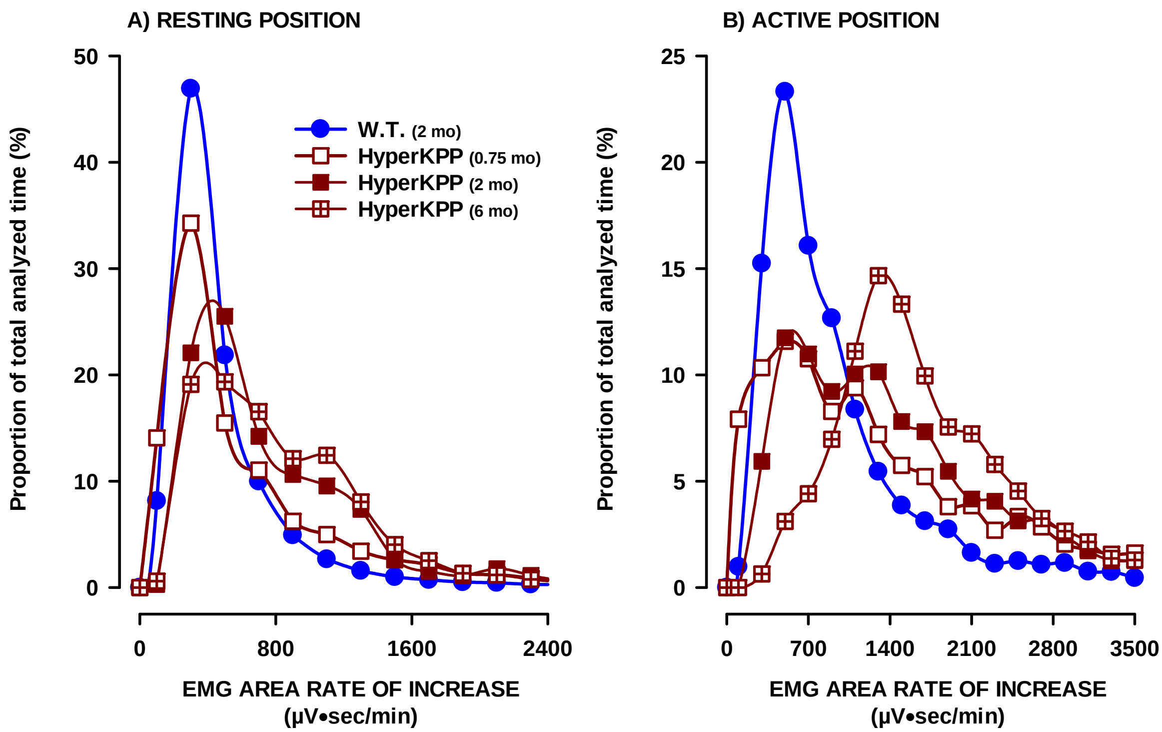


**Figure 3-6. Frequency distribution of the rate of increase of the area under the EMG curve is shifted towards larger values in 24 week old HyperKPP mice for both A) resting and B) active mice.** Rates of increase were separated into bins of 200 µV*sec/min, calculated as described in the text, and the amount of time for each rate bin was expressed as a % of the total time analyzed. WT curve is shown for reference. Mice used were 3, 8 and 24 weeks old (n=5)

animals respectively. For 3 week old animals, the curve was shifted towards the left, with values closer to those seen in the WT mice. In the 3 week mice, there was a relatively high frequency of values in the 0 – 200 μV•sec per min range, occurring 13% of the time, where these values did not occur at all in older HyperKPP mice. Additionally, the value of the slope was between 400 and 600 μV•sec per min nearly 35% of the time in 3 week animals, much higher than in older HyperKPP mice, and more similar to the values for WT. Furthermore, the shape of the 3 week curve is remarkably similar to that of WT mice, with a sharp peak followed by a relatively quicker decline than in other age groups, albeit the decline is more gradual than in WT. However, there is still more activity in 3 week animals in ranges greater than 1000 in 3 week HyperKPP mice relative to WT, with frequencies of 30% and 10% respectively. Regardless, there is still more activity in the higher ranges in 8 and 32 week mice than seen in the 3 week old animals.

When considering the active portion of the EMG traces, there was more variability across the different age groups. For 3 week animals, there was no peak at all in the curve, simply a large plateau (Fig 3-6) Once again, for the 3 week animals, slope values in the 0 – 200 μV•sec per min range were observed, at a frequency of 8%, where no such values were observed for other ages of HyperKPP mice. Other than an increase in values lower than 600 μV•sec per min, the 3 week curve is very similar to the 8 week curve. For 24 week animals, the peak value is shifted to the right, towards larger values, at 1400 μV•sec per min, compared to 600 μV•sec per min for the 8 week animals. The 24 week curve has a different shape than that of the 3 and 8 week animals, with a peak in the mid-range, and a gradual rise and decline up to the slope. Overall, there was a larger frequency of observing values greater than 1400 μV•sec per (60%) relative to 8 week old animals where this frequency was closer to 50%. From the shape of the curves, it would seem that it is possible there is some worsening in symptoms from 8 weeks to 24 weeks, as the peak values for when mice were active are for higher slope values in the 24 week animals than at any other age.

When considering the total area under the curve for the resting position, the average total areas under the curve were: 7228μV·sec, 8690μV·sec, and 8700 μV•sec, for 3, 8 and 32 week old HyperKPP mice, for a 10 min period (Fig 3-7). For time spent while active, the total average areas under the curve were: 25086 μV•sec, 19234μV·sec, and 19374 μV•sec, for 3, 8 and 24 week old mice. It is interesting to note that the area under the curve is much higher in the active 3 week mice than would be anticipated when considering the greatly decreased slope values seen previously in figure 3-6. Also of interest to note is that the average area under the curve is nearly identical in all cases between the 8 and 32 week animals, despite the slope curves suggesting that the 32 week animalsare more affected.

## 3.2 - CHARACTERISTICS OF FDB SINGLE FIBERS

The original objective was to measure changes in $[Ca^{2+}]_i$ and channel activity that can be affected by an increased $[Ca^{2+}]_e$. Single muscle fibers are the preferred method for such measurements, especially intracellular ion concentrations, such as $Ca^{2+}$. Single muscle fibers from the FDB muscle are readily obtained, and are very stable, whereas it is very difficult to obtain viable fibres from soleus and EDL muscles. Considering the HyperKPP symptoms, there were several expectations of dysfunction in HyperKPP fibers, including the possibility of supercontracted fibers, fibers which have become unviable as a result of extreme shortening, and fibers contracting spontaneously as a result of myotonic discharge. Additionally, a higher threshold for activation

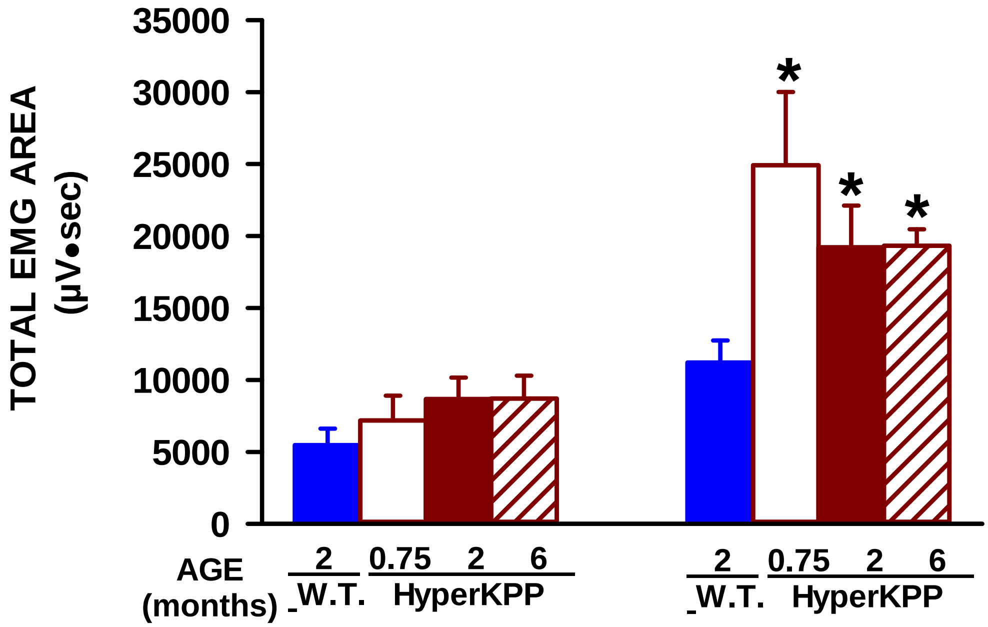


**Figure 3-7. The mean total area under the EMG traces was higher in HyperKPP animals that were (left) resting and (right) active.** The total area was calculated for each mouse and then averaged. Vertical bars represent SE of 5 mice.

***** Significantly different from wild type muscle, ANOVA and L.S.D., $P < 0.05$.

was very likely as a result of the fibers having potential to be completely depolarized, leading toa higher number of non – contracting fibers, or even paralysis. Therefore, in a first series of experiments, single FDB fibers were obtained from both WT and HyperKPP mice to determine the contractile characteristics of individual fibers. Single muscle fibers from HyperKPP FDB muscles were successfully obtained, and surprisingly, there was no evidence of supercontracted or spontaneously contracting HyperKPP fibers. HyperKPP fibers were indistinguishable from WT fibers. In addition, the number of contracting fibers and the stimulation strength relationship was the same for WT and HyperKPP fibers, whether expressed as a percentof total fibers, or total contracting fibers, with approximately 70% of all WT and HyperKPP fibers contracting (Fig 3-8). Thus, single muscle fibers from HyperKPP FDB muscles did not show any outward signs of the disease pathology.

### 3.3 $K^+$ SENSITIVITY AND FORCE MEASUREMENTS IN FDB MUSCLES

This leads to the possibility that the FDB muscle is not affected by HyperKPP as observed with the diaphragm (Barbalinardo and Renaud, unpublished) as opposed to the EDL and soleus (Lucas, 2012). It is well documented that human patients with HyperKPP show hypersensitivity to elevated $K^+$, which was also reported for mouse EDL and soleus muscles (Hayward et al., 2008). This hypersensitivity consists of a much larger reduction in force produced when exposed to elevated $[K^+]_e$. Therefore, to further determine the extent to which the FDB muscle is affected in HyperKPP mice, the effects of increasing $[K^+]_e$were tested using FDB muscle bundles.

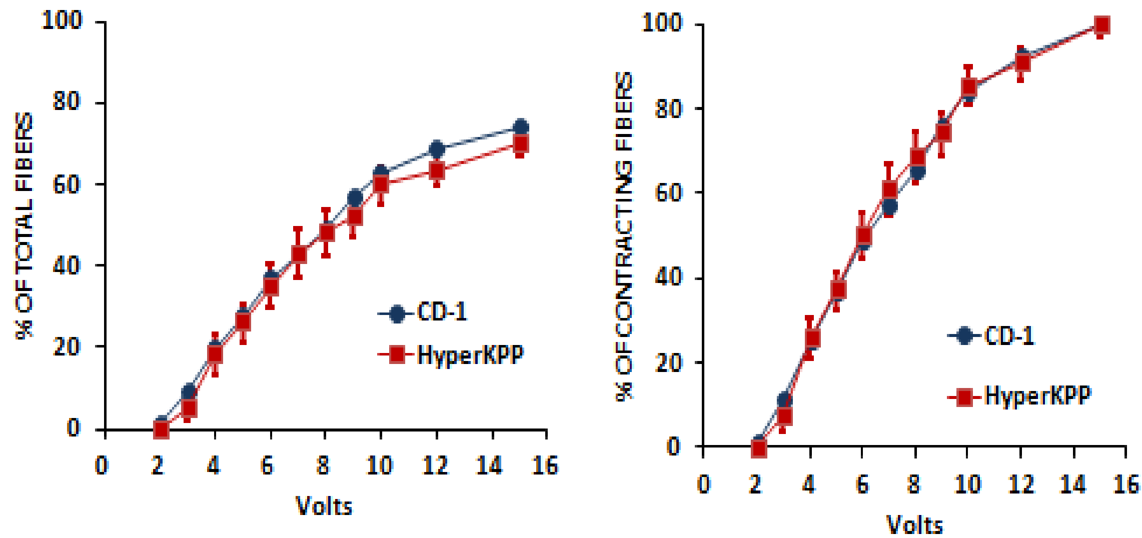


**Figure 3-8. The contraction threshold and stimulation strength relationship was indistinguishable between WT and HyperKPP FDB single fibers.** A) The number of fibers contracting at different stimulation strengths was expressed as a percentage of the total number of fibers. B) The number of fibers contracting at different stimulation strengths expressed as a percentage of total contracting fibers. Vertical bars represent the SE of 7 WT and 5 HyperKPP mice.

Again, no difference in contractile characteristics between WT and HyperKPP FDB muscles were observed. There were no differences in the force generated prior to exposure to $K^+$ in WT and HyperKPP muscles at either 1.3 mM $Ca^{2+}$,(27 and 31 N/cm$^2$,respectively), or at 4 mM $Ca^{2+}$, (32 and 31 N/cm$^2$ respectively). For both WT and HyperKPP FDB, an increased in $[K^+]_e$ to 11 mM reduced tetanic force to 18 N/cm$^2$, representing a decrease, which was the same regardless of the $[Ca^{2+}]_e$ (Fig 3-9). Taken together, the force generation, potassium sensitivity, voltage activation of single fibers indicate that the HyperKPP FDB muscle is not affected by the defective $Na_V1.4$ channels. Therefore, a new approach to study the mechanism of action of $Ca^{2+}$ had to be undertaken.

**3.4 - CALCIUM UPTAKE:**

One potential mechanism for the $Ca^{2+}$-induced symptom alleviation involves the activation of BK channels allowing a $K^+$ efflux, which act to hyperpolarize the cell membrane. In order for the BK channel to be activated, $[Ca^{2+}]_i$ must increase. Any increase in $[Ca^{2+}]_i$ is likely to depend on increased $Ca^{2+}$ influx, as $[Ca^{2+}]_e$ is increased. The $Ca^{2+}$ influx can be through either $Ca_V1.1$channels themselves as the membrane depolarizes, or through the $Na_V1.4$ channel (Gissel and Clausen, 2000).Gissel and Clausen successfully measured an increased $Ca^{2+}$ influx when muscles were active. Myotonic discharge is a form of activity seen in HyperKPP muscles.$Ca^{2+}$ influx was measured while muscles were unstimulated and exposed to 4.7 mM $K^+$. To determine if some of the $Ca^{2+}$ is entering via the $Na_V1.4$ channel, influx was also measured in the presence and absence of TTX, a blocker of the $Na_V1.4$ channel. EDL and soleus muscles were used because previous experiments have shown that these two muscles are both highly affected by HyperKPP in the mouse model (Hayward et al., 2008)

A) B)

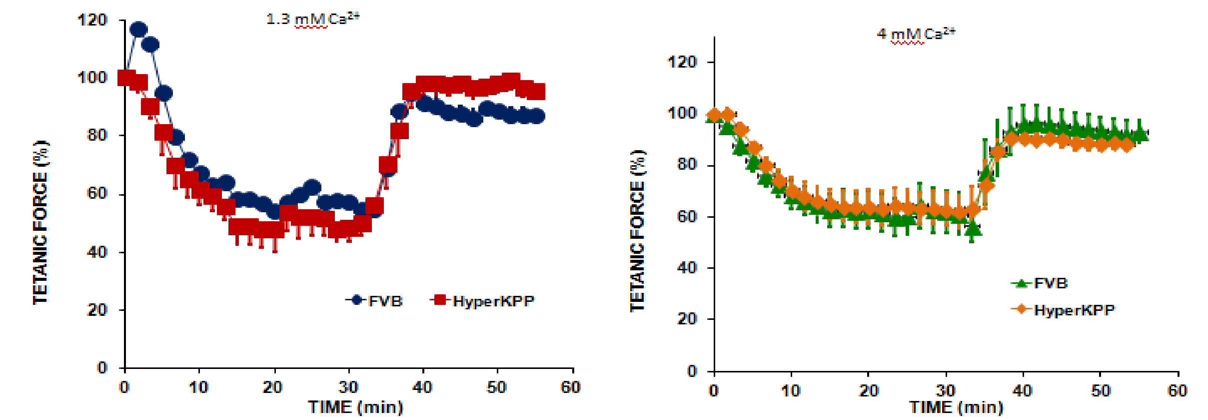


**Figure 3-9. HyperKPP FDB had a similar $K^+$ sensitivity when compared to WT.** At time 0, muscles were switched from $[K^+]$ of 4.7 mM to 11mM $K^+$ while $[Ca^{2+}]_e$ was A) 1.3 mM and B) 4.0 mM. Muscles were returned to control $[K^+]$ at 35 min. Peak tetanic force is expressed as a percentage of the force maximum at 4.7mM $K^+$. Vertical bars represent SE of 5 muscles.

There was no difference in $Ca^{2+}$ influx between WT and HyperKPP muscles whether TTX was present or not. In WT EDL, $Ca^{2+}$ influxes were 40 and 41 μmole/g muscle tissue in the absence and presence of TTX. In HyperKPP EDL the vales were 51 and 54 μmole/gmuscle respectively, but this was not significantly different from WT (Figure 3-10). The situation was the same in WT soleus muscle, with $Ca^{2+}$ influxes of 42 and 47 μmole/gmuscle tissue for TTX treated muscles and untreated muscles respectively. In HyperKPP soleus muscles, there was a decrease observed between muscles exposed to TTX, with influxes reported of 52 and 32 μmole/g muscle tissue respectively.

Previous studies have established that when exposed to 11 mM $K^+$$Na_V$1.4 channels with HyperKPP mutations can go into a non – inactivating mode, leading to increased $Na^+$ influx, myotonia, and eventually paralysis. (Cannon etal., 1991, Hayward et al., 2008). Therefore, $Ca^{2+}$ influx was also measured at 11 mM $K^+$. It was found that there were no signifcant differences at any concentration of $K^+$ between any muscles. In WT EDL, the $Ca^{2+}$ influxes at 4.7 mM and 11mM $K^+$ were 150 and 167 nmol/g/min respectively (Fig 3-11). In HyperKPP EDL, the $Ca^{2+}$influxes at 4.7 mM and 11 mM $K^+$ were 144 and 158 nmol/g/min respectively. In WT soleus, the $Ca^{2+}$influxes at 4.7 mM and 11 mM $K^+$ were 191 and 211 nmol/g/min respectively. In HyperKPP soleus,the $Ca^{2+}$ influxes at 4.7 mM and 11 mM $K^+$ were 212 and 183 nmol/g/min respectively. In all but the HyperKPP soleus muscle, there was a trend towards slightly increased $Ca^{2+}$ influx at the elevated $K^+$ concentration. These results do not provide evidence for an activation of BK channels associated with an increased $[Ca^{2+}]_i$ when $[Ca^{2+}]_e$ increases (see discussion for further details).

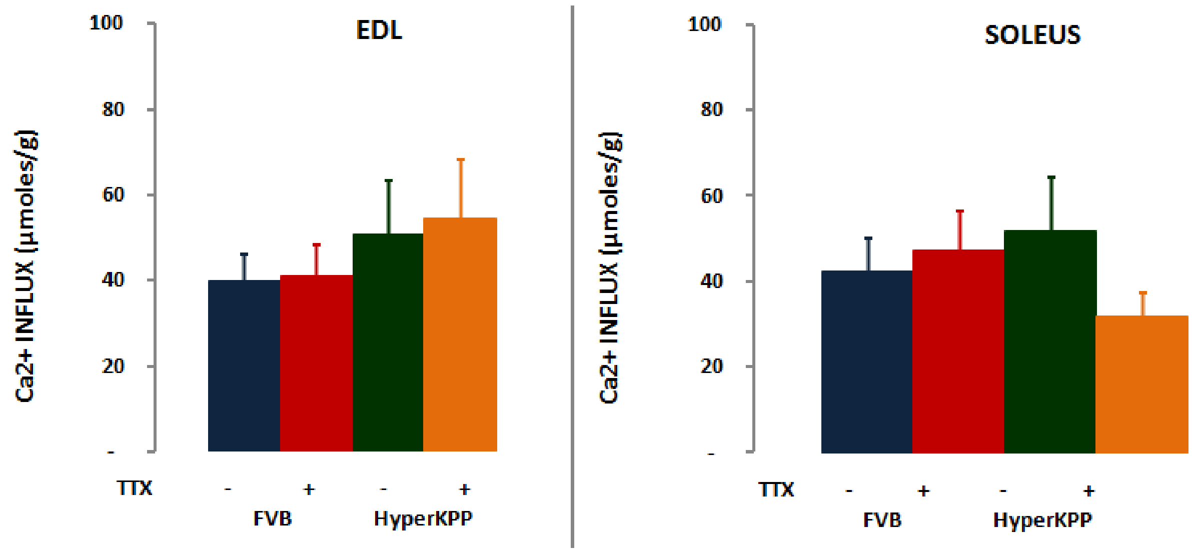


**Figure 3-10. At 4.7 mM $K^+$, $Ca^{2+}$ influx in A) EDL and B) Soleus were similar in WT and HyperKPP mice.** Following an equilibrium period, muscles were exposed to 2µCi/ mL $^{45}Ca$ for 15 minutes, with or without 100 nM TTX. $Ca^{2+}$ influx is shown in µmol/gram of wet weight muscle tissue. Vertical bars represent SE of 5 muscles.

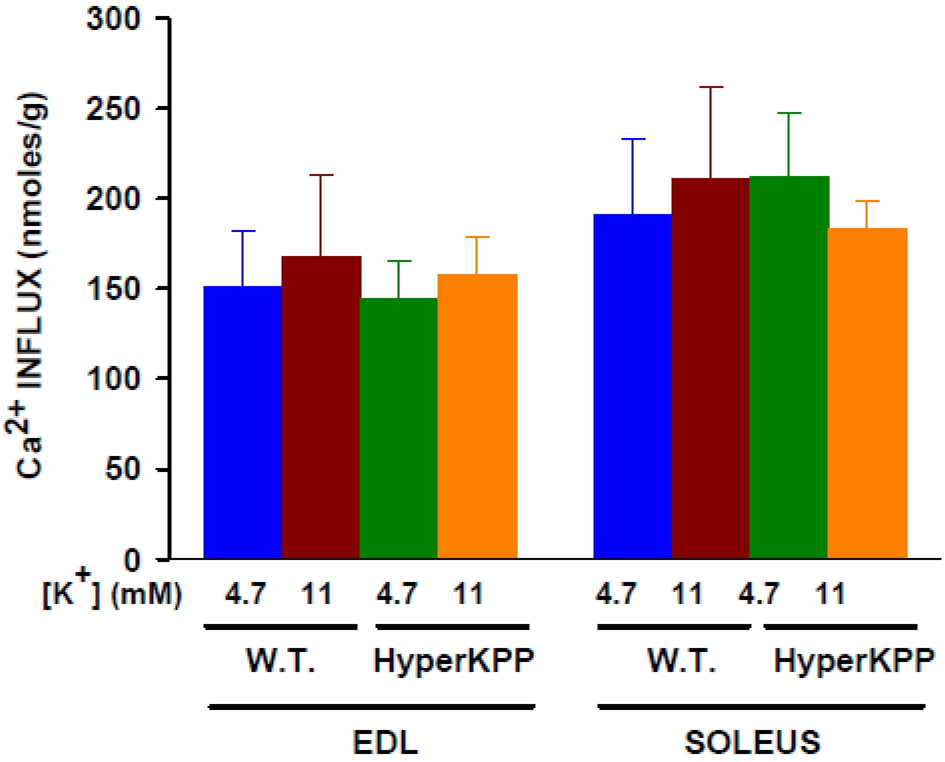


**Figure 3-11: At 11 mM $K^+$, $Ca^{2+}$ influx in A) EDL and B) Soleus were similar in WT and HyperKPP mice**. Following an equilibrium period, muscles were exposed to 2μCi/ mL $^{45}Ca^{2+}$ for 15 minutes, at either 4.7 (control conditions) or 11 mM $K^+$. Vertical bars represent the standard error (S.E.) of 5 muscles. No significant difference, ANOVA P > 0.05.

### 3.5 - $Na^+$ INFLUX:

Another potential mechanism for $Ca^{2+}$ to be alleviating HyperKPP symptoms is via a direct effect on the increased $Na^+$ window current from the mutated $Na_V1.4$.Thus, in order to investigate whether increasing the $[Ca^{2+}]_e$ could potentially reduce the persistent $Na^+$ influx, we measured $Na^+$ at two $[Ca^{2+}]_e$ ,1.3 and 4 mM. At 1.3 mM $Ca^{2+}$, HyperKPP EDL and soleus muscles had an increased TTX sensitive $Na^+$ influx when compared to WT muscles (Fig 3-12). $Na^+$ influx in WT EDL was 538 nmoles/g/min, and 328 nmoles/g/min in TTX treated muscles. For HyperKPP EDL muscles the respective values were 958 nmoles/g/min, and 528 nmoles/g/min. Therefore, the TTX sensitive $Na^+$ influxes were 210 and 430, and this influx is much higher in HyperKPP EDL. For soleus muscles, the TTX sensitive $Na^+$ influxes were 89 and 327 nmoles/g/min for WT and HyperKPP respectively, once again much larger in the HyperKPP muscle. It is clear that at 1.3 mM $Ca^{2+}$ that there is a much larger amount of $Na^+$ influx in diseased muscles.

However, in HyperKPP muscles in the absence of TTX exposed to 4 mM $Ca^{2+}$, $Na^+$ influxes were significantly reduced to levels similar to those of WT muscles (Fig 3-13). Furthermore, the addition of TTX no longer resulted in significant lowering of $Na^+$ influx. At 4.0 mM $Ca^{2+}$, the TTX sensitive $Na^+$ influxes in EDL muscles were 179 and 66 nmoles/g/min for WT and HyperKPP muscles. At elevated $Ca^{2+}$ the TTX sensitive $Na^+$ influx is reduced in both WT and HyperKPP muscles, but is reduced much further in HyperKPP muscles (430 vs. 66 nmoles/g/min). In soleus muscles, this trend continues, with TTX sensitive influxes of 107 and 76 nmoles/g/min, for WT and HyperKPP muscles respectively. Again, this is a significant reduction compared to muscles exposed to 1.3 mM $Ca^{2+}$.There is a clear decrease in $Na^+$ influx

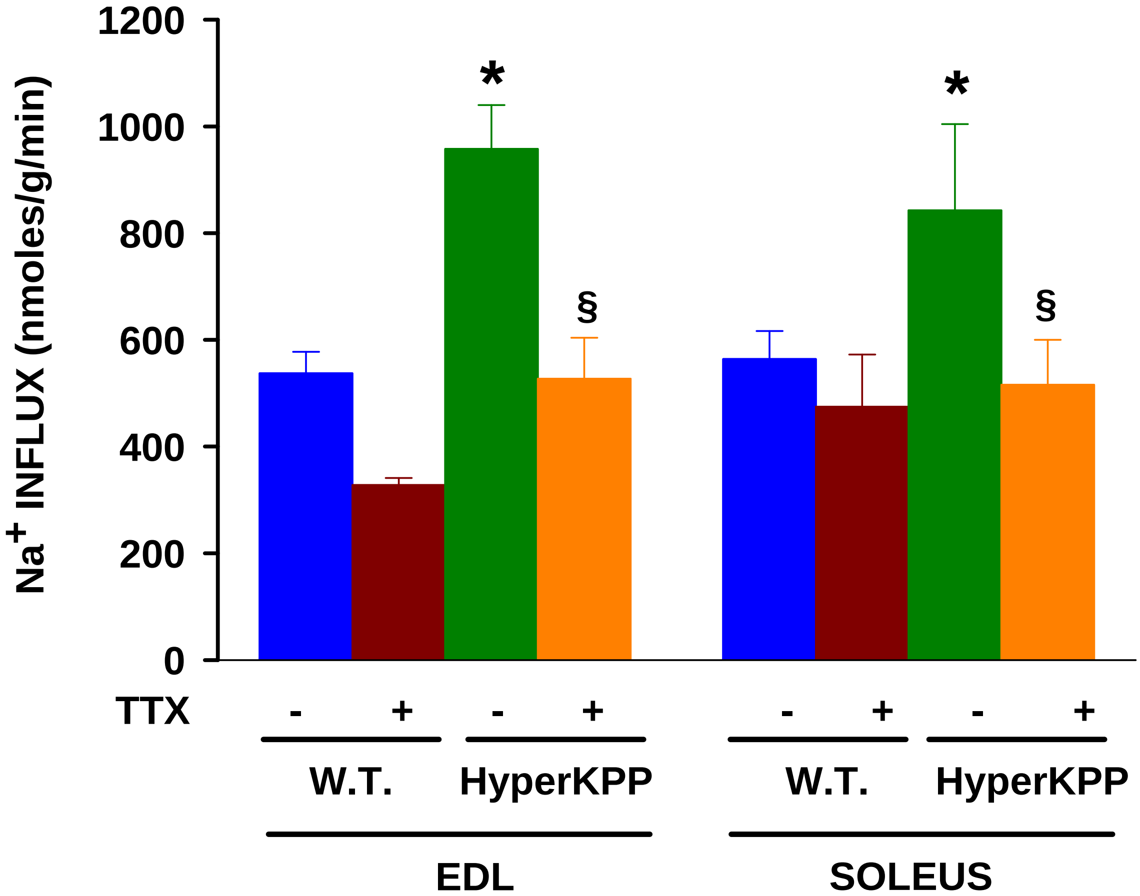


**Figure 3-12. At 1.3 mM $Ca^{2+}$ TTX sensitive $Na^+$ influx was greater in HyperKPP EDL and soleus.** Muscles were exposed to 2 μCi/ mL $^{22}Na^+$ for 10 minutes, with or without 500 nM TTX. Vertical bars represent the S.E. of 5 muscles.

* Significantly different from wild type muscle.

§Significantly different from no TTX, ANOVA and L.S.D. , $P < 0.05$.

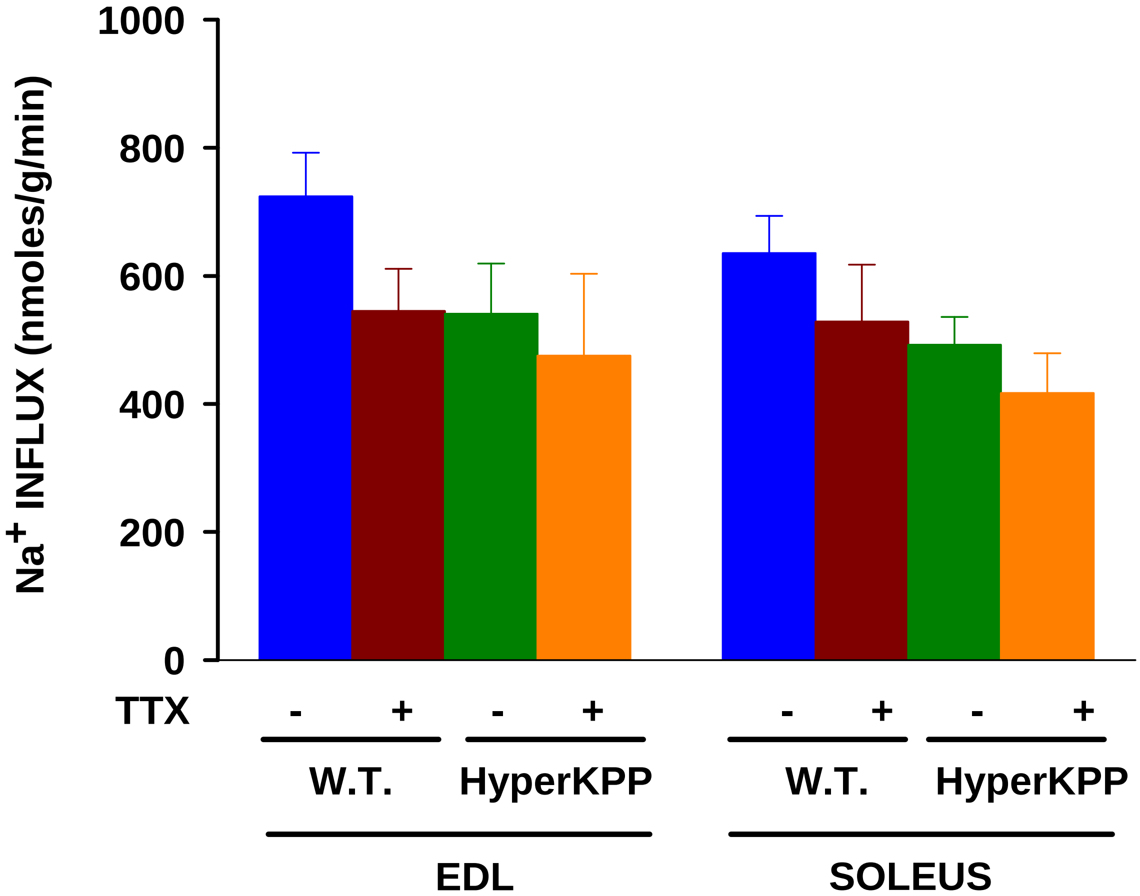


**Figure 3-13. At 4.0 mM $Ca^{2+}$, TTX sensitive $Na^{+}$ influx was not significantly different between HyperKPP and wild type muscles.** Following an equilibrium period, muscles were exposed to 2 µCi/ mL $^{22}Na^{+}$ for 10 minutes, with or without 500 nM TTX. Vertical bars represent the S.E. of 5 muscles. No significant difference, ANOVA P > 0.05.

in the diseased muscles compared to the control level of $Ca^{2+}$, with a complete abolishment of the aberrant influx caused by the defect in slow inactivation of the $Na_V1.4$.

Finally, in order to determine whether the effect $Ca^{2+}$ was having on the $Na^+$ was through a divalent cation effect. Divalent cations are known to have a ‘shielding’ effect on the $Na_V$, this reducing some of the influx (Woodhull, 1973, Frankenhaeuser and Hodgkin, 1957). In order to test for this, $Na^+$ influx was measured in muscles exposed to an elevated concentration of $Mg^{2+}$, 5.8 mM, as opposed to the control of 3.1 mM, a difference that is equivalent to the change from 1.3 to 4 mM $Ca^{2+}$. HyperKPP muscles that were exposed to elevated $Mg^{2+}$ did show some reduction in $Na^+$ influx, though not to the same degree as with elevated $Ca^{2+}$ (Fig 3-14). For EDL muscles exposed to elevated $Mg^{2+}$, the TTX sensitive influxes were 70 and 202 nmoles/g/minfor WT and HyperKPP muscles, respectively. While the reduction is not as complete as when exposed to 4 mM $Ca^{2+}$, there is still a reduction in TTX sensitive $Na^+$ influx compared to control $Ca^{2+}$conditions.(430 v 202 nmoles/g/min). For soleus muscles, the TTX sensitive influxes were 85 and 340, for WT and HyperKPP muscles respectively. Therefore, the reduction in $Na^+$ observed at 4.0 mM $Ca^{2+}$does not occur in soleus muscle exposed to elevated $Mg^{2+}$, as the influxes at elevated $Mg^{2+}$, 340, and 1.3 mM $Ca^{2+}$,327, are very similar. It is therefore unlikely that divalent cation shielding is the only mechanism through which $Ca^{2+}$ alleviates the excess $Na^+$ influx in HyperKPP muscle.

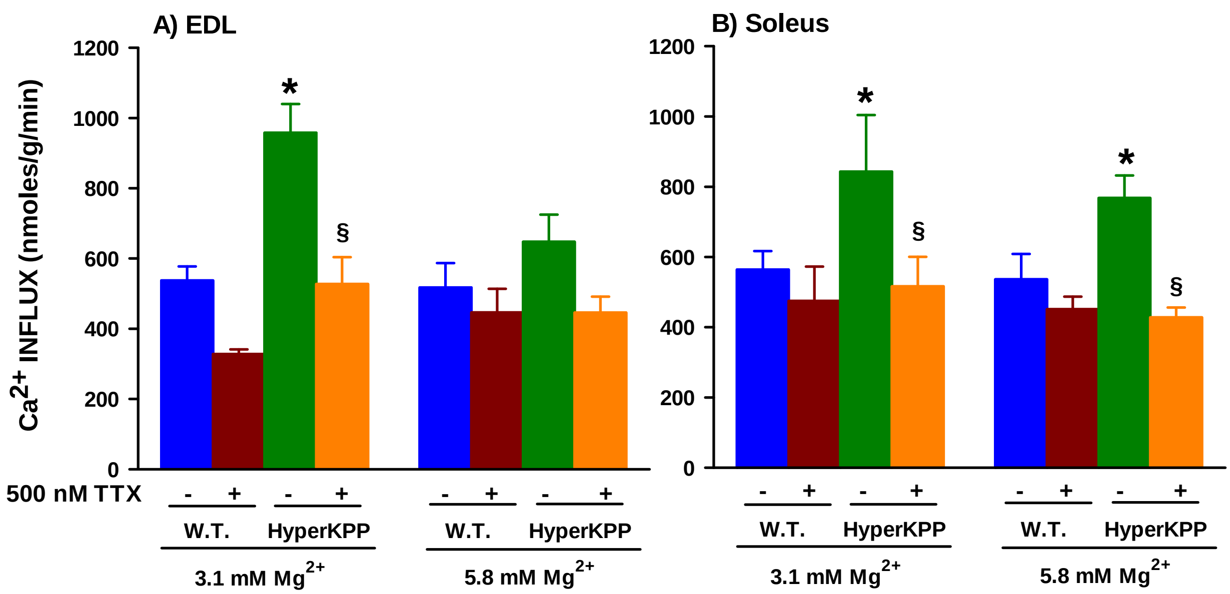


**Figure 3-14. 5.8 mM $Mg^{2+}$ reduced TTX sensitive $Na^{+}$ influx in HyperKPP EDL but not soleus.** Muscles were exposed to 1.3mM $Ca^{2+}$ and either at 3.1 (control) or 5.8 mM $Mg^{2+}$; i.e., to increase [$Mg^{2+}$] by the same amount as [$Ca^{2+}$] from 1.3 to 4.0. Vertical bars represent the S.E. of 5 muscles.

* Significantly different from wild type muscle.

§Significantly different from no TTX, ANOVA and L.S.D. , $P < 0.05$.

# CHAPTER 4: DISCUSSION

The major findings of this study are: 1) the contractile characteristics of HyperKPP FDB single fibers did not differ from those obtained from WT FDB muscles; 2) HyperKPP FDB muscles were not more susceptible to increased $[K^+]_e$ and produced just as much force as their WT counterparts; 3) $Ca^{2+}$ influx was not increased in HyperKPP EDL or soleus muscles; 4) TTX sensitive $Na^+$ influx was much higher in HyperKPP EDL and soleus than in WT muscles; 5) At 4 mM $Ca^{2+}$, TTX sensitive $Na^+$ influx was greatly reduced in HyperKPP EDL and soleus, such that there is no difference in influx between HyperKPP and WT muscles; 6) Elevated $Mg^{2+}$ did not reduce the TTX sensitive $Na^+$ influx to the same extent as elevated $Ca^{2+}$ in HyperKPP EDL and soleus; 7) EMG measurements were successfully used to measure myotonia in HyperKPP mice *in vivo*; 8) In 8 week old HyperKPP mice, there was increased electrical activity both in the resting position and when mice were active; 9) There is some worsening of symptoms as HyperKPP mice age, according to EMG data.

### 4.1 EMG MEASUREMENTS

The main objectives of the EMG measurements were to develop a method to quantify the symptoms of myotonia and paralysis experienced by HyperKPP mice, as well as determine how the symptoms progress as the animals age. For this study, EMG data was accumulated over a period of four hours for each animal used. This was done to increase the chances of an HyperKPP mouse having a paralytic attack during the experiment. Unfortunately, none of the mice tested experienced paralysis while the EMG electrodes were in place, despite all HyperKPP mice having been previously reported to have experienced paralytic attacks by animal care technicians. This is very likely due to the very short (10-30 sec) duration of the attacks and the high variability in the disease as reported in humans with regard to the occurrence of paralytic attacks. This study shows that the incidence of myotonia is also highly variable between HyperKPP mice. The high variability was especially evident in the EMG data, as can be seen when the WT traces, which are all very similar, are contrasted with those of the individual HyperKPP animals which were highly variable (Appendix 2). This variability is also in agreement with the studies by Lucas (2012), in which HyperKPP muscles were tested in vitro demonstrating a large variety of reactions, from being similar to WT muscles, to high levels of force development or spontaneous contractions in the absence of electrical stimulation due to myotonic discharges, to complete paralysis.

It is very clear from the results that at 8 weeks of age, there is a large increase in EMG activity in HyperKPP animals, both in the resting position and when the animals are active. EMG is a measure of the summation of action potentials in the muscle, it can be concluded that there is additional action potential generation in HyperKPP animals compared to their WT counterparts, as they are experiencing myotonic discharges, one of the major symptoms of the disease.

Hayward et al. (2008) also reported using EMG electrodes myotonic activity in HyperKPP mice; however, the myotonic discharges were observed in response to a movement of the electrode. The difficulty with the Hayward study is that the measurements were carried out with anesthetized mice and this study clearly demonstrated that all EMG activity fell to zero in both HyperKPP and W.T. mice. Furthermore, none of the EMG signals reported in this study can be related to electrode displacements when mice moved around, because no electrical activity could be measured when legs were moved by hand while mice were under anesthesia. Therefore, this study has clearly demonstrated that it is possible to measure extent to which myotonia is being experienced, *in vivo*. In future studies it will be possible to test new pharmacological approaches to treat HyperKPP in these mice using this technique.

### 4.2 EMG ACROSS DEVELOPMENT

EMG measurements were also carried out as part of a larger study to help understand the progression of the disease across the lifespan of the mice. At all ages, HyperKPP gastrocnemius had more electrical activity than the WT muscles, both in the resting position and while animals were active. The differences between resting W.T. and HyperKPP mice were less at 3 weeks of age than at 2 and 6 months of age. However, when active, 3 week HyperKPP mice had the largest total area under the curve. This is consistent with other studies completed that suggest that there is no major worsening of symptoms after 3 weeks of age (Lucas 2012, Khogali 2012).

### 4.3 HYPERKPP FDB MUSCLES HAVE NO SYMPTOMS

Previous *in vitro* studies have shown substantial force depression and paralysis in HyperKPP EDL and soleus muscles (Lucas, 2012). It was therefore expected that single fibers obtained from HyperKPP FDB muscles would either, be contracting spontaneously or supercontracting, due to myotonic discharge. Higher activation threshold was also expected in fibers with partial loss of membrane excitability or full paralysis. None of these characteristics were observed.

To verify that the apparent lack of symptoms was not related to the fact that single fibers are well superfused preventing any accumulation of extracellular $K^+$, FDB muscle bundles were also tested*in vitro*. HyperKPP FDB muscles produced as much peak tetanic force as their WT counterparts, whereas HyperKPP EDL did not, generating only 34% of the force of WT muscles. Furthermore, HyperKPP FDB had a similar $K^+$sensitivity as WT FDB, whereas HyperKPP EDL showed a loss of 88% of force (Hayward et al., 2008). Therefore, whole HyperKPP FDB muscles did not show any HyperKPP symptoms, much like the single fibres. Finally, contrary to EDL and soleus, for which there are significant changes in fiber type towards more type IIA fibers, no such changes was observed for HyperKPP FDB (Khogali, 2012). This suggests that even *in vivo* HyperKPP FDB has no symptoms. All together, these data suggest that the FDB, like the diaphragm, is spared of HyperKPP symptoms. The reason for which the diaphragm remains unaffected needs to be elucidated in future studies. However, one explanation for the lack of symptoms in FDB is that compared to EDL, soleus and diaphragm, HyperKPP FDB contained the lowest Nav1.4channel protein content and the lowest TTX-sensitive $Na^+$ influx (Ammar and Renaud, unpublished results).

## 4.4$Ca^{2+}$ UPTAKE:

In order to study the benefits of $Ca^{2+}$ in HyperKPP muscle, the EDL and soleus muscles must be used instead, as single fibers were no longer a viable method for investigation. As per the overall hypothesis given in the introduction, one mechanism through which an increase in $[Ca^{2+}]_e$may be alleviating symptoms in HyperKPP muscles is via an activation of BK channels, which are voltage and calcium sensitive $K^+$ channels that aid in repolarizing the cell membrane.

This would counteract the depolarization caused by the persistent $Na^+$ influx found in HyperKPP muscles. In order for the BK channel to be involved, there must be an increase in $[Ca^{2+}]_i$ to trigger opening of the channel; the latter being due to increases in (1) $Ca^{2+}$ entering via the L-type $Ca^{2+}$ channels themselves, ($Ca_V1.1$) or (2)$Ca^{2+}$ entering via the $Na_V1.4$ channels upon depolarization **(**Gissel and Clausen , 2000).So, as a first step,$^{45}Ca^{2+}$influx was measured, except that the experiments had to be carried out using HyperKPP EDL and soleus since the FDB is not affected by symptoms.

No difference in $^{45}Ca^{2+}$uptake was observed between WT and HyperKPP EDL or soleus muscles. These results were observed at both 1.3 and 4.0 mM $Ca^{2+}$and at both 4.7 mM $K^+$ or at 11 mM $K^+$, a concentration known to exaggerate HyperKPP symptoms in EDL and soleus muscles. In unstimulated WT muscles,$^{45}Ca^{2+}$ uptake were expected to be very small through $Ca_V1.1$ and Nav1.4 because there is very little flux of $Ca^{2+}$ at rest in healthy muscle (Gissel and Clausen, 1999). An increased $^{45}Ca^{2+}$influxwas expected in HyperKPP muscles because of the myotonic discharge allowing an influx through either Cav1.1or the defective Nav1.4channels when the membrane depolarizes. Therefore, this study provided no evidence for any greater $Ca^{2+}$ uptake in HyperKPP muscles. Consequently, it provides no evidence for any increases in $[Ca^{2+}]_i$ when $[Ca^{2+}]_e$ is increased and consequently it appears unlikely that BK channels become activated; i.e., the BK channel may not be the mechanism by which $Ca^{2+}$ alleviates HyperKPP symptoms.

One argument against this conclusion would be that the $^{45}Ca^{2+}$uptake were too small to be sensitive enough to obtain differences between W.T. and HyperKPPmuscles. This might be quite important because only a very local increase in $[Ca^{2+}]$ just under the cell membrane might be enough to activate BK channels. So, to answer the question as to whether BK channels are involved in the protective effect of $Ca^{2+}$ will be in future studies to measure$[Ca^{2+}]_i$ with $Ca^{2+}$ indicators and BK channels activity in HyperKPP muscles under different $[Ca^{2+}]_e$. While these experiments were planned for this study (see aims in Introduction), they could not be carried out because one required the isolation of single fibers for such measurements and healthy single fibers can only be obtained from unaffected FDB muscles.

### 4.5 $Na^+$ INFLUX

A second mechanism hypothesized in the introduction regarding how$Ca^{2+}$ may alleviate symptoms in HyperKPP patients is via a direct reduction in $Na^+$ influx through the defective $Na_V1.4$ channels. At 1.3 mM $Ca^{2+}$, TTX sensitive $Na^+$ influx was much higher in HyperKPP EDL and soleus as reported. Interestingly, when $[Ca^{2+}]_e$ was raised to 4 mM, the TTX sensitive $Na^+$ influx in HyperKPP EDL and soleus were no longer different compared to those in WT muscles. This suggest that $Ca^{2+}$significantly reduced the excessive $Na^+$ influx and thereby reduces myotonic discharge and the subsequent paralysis as shown in Fig 1-9.

The next question was how exactly is $Na^+$ influx reduced by $Ca^{2+}$. It is known that $Ca^{2+}$, like other divalent cations, has a shielding effect on the membrane, which tends to prevent other cations from penetrating the membrane (Gissel and Clausen, 1991). To test this possibility, the effect of increasing the concentration of another divalent cation, $Mg^{2+}$, on $Na^+$ influx was determined. Increased $[Mg^{2+}]_e$ was partially effective in reducing the TTX sensitive $Na^+$ influx in HyperKPP EDL, but not at all effective in HyperKPP soleus muscles. Therefore, it is unlikely that the mechanism through which $Ca^{2+}$ reduces $Na^+$ influx is entirely due to a divalent cation shielding effect.

Another possible mechanism by which $Ca^{2+}$ may reduce $Na^+$ influx is a shift in the voltage relationship of activation of the $Na_V1.4$ towards less negative potentials (Hanin and Campbell, 1983). This would directly counteract the opposite shift in the voltage relationship of activation in HyperKPP, which is shifted towards more negative potentials. It has also been shown that increasing $Mg^{2+}$ concentration has a similar effect on the membrane, directly affecting the gating charge - voltage relationship, and shifting it to less negative potentials, however this effect is not as strong as with increased $[Ca^{2+}]$ (Hanin and Campbell, 1983). This may explain why $Mg^{2+}$ was not as effective as $Ca^{2+}$ in reducing the TTX sensitive $Na^+$ influx in HyperKPP soleus muscle.

When considering the $Na^+$ influx results alone, it would seem that 4 mM $Ca^{2+}$ completely abolishes the symptoms in HyperKPP muscles. However, we know that $Ca^{2+}$ alone is insufficient as a treatment for HyperKPP, and even though HyperKPP muscles that are exposed to 4 mM $Ca^{2+}$ have greater force production and resistance to 11 mM $K^+$ than HyperKPP muscles exposed to 1.3 mM $Ca^{2+}$, they still do not produce the same amount of force as WT muscles (Lucas, 2012). Therefore, there must be other factors at work in HyperKPP muscle. Overall, it was found that 4 mM $Ca^{2+}$ is very effective in reducing the abnormal TTX sensitive $Na^+$ influx in HyperKPP EDL and soleus muscles, however the exact mechanism through which this is achieved is still unknown. Future studies could elucidate this mechanism.

## 4.6 SUMMARY:

In conclusion, this study clearly demonstrated that the primary symptom of the M1592V HyperKPP mouse model is extra electrical activity possibly due to myotonic discharge as observed from the EMG measurements, while contrary to human the paralytic attacks are rare and very short in duration. Furthermore, the extra electrical activity can be observed within 3 weeks of age at a time when the $Na^+$ channel content and TTX-sensitive $Na^+$ influx have reached maximum suggesting the HyperKPP symptoms are solely related to the defective Nav1.4 channels and not from other changes in the content of activity of other membrane components worsening the symptoms. This conclusion is in agreement with those presented by Lucas (2012) and Khogali (2012).

This study also demonstrated that not all HyperKPP muscles are affected by the disease as FDB muscles showed no sign of sudden contractions (myotonic discharge) or elevated $K^+$sensitivity (paralysis). For this muscle, the reason for the lack of symptoms might be due to very low Nav1.4 channel expression and TTX-sensitive $Na^+$ influx. Finally, no evidence was obtained to support an activation of BK channels as a mechanism by which $Ca^{2+}$ reduces HyperKPP symptoms. A major effect appears to be a reduction in $Na^+$ influx through the defective Nav1.4 channels but the mechanism of this effect remains to be determined.

# CHAPTER 5: REFERENCES


Armstrong, CM, Bezanilla, F. Inactivation of the sodium channel. II. Gating current experiments. *J Gen, Physiol.* 70: 567-590, 1997.

Berchtold, M, Brinkmeier, H and Muntener, M. Calcium ion in skeletal muscle: its crucial role for muscle function, plasticity, and disease. *Physiological Reviews* 80: 1215-1265, 2000.

Boudreault L, Cifelli C, Bourassa F, Scott K and Renaud J.M. Fatigue preconditioning increases fatigue resistance and reduces muscle dependency on KATP channels to prevent contractile dysfunctions in mouse FDB. *J Physiol (Lond.)* 588:4549–4562, 2010.

Bradley WG, Taylor R, Rice DR, Hausmanowa – Petruzewicz I, Adelman LS, Jenkison M, Jedrzejowska H, Drac H and PendleburyWW.Progressive myopathy in hyperkalemic periodic paralysis.*ArchNeuro*l 47: 1013-1017, 1990.

Cannon SC. Pathomechanisms in channelopathies of skeletal muscle and brain. Annu*Rev Neurosci* 29, 387-415. 2006

Cannon SC, Brown RH and Corey DP. Theoretical reconstruction of myotonia and paralysis caused by incomplete inactivation of sodium channels.*Biophys J* 65: 270-288, 1993.

Cannon SC, Brown RH and Corey DP. A sodium channel defect in Hyperkalemic periodic paralysis: potassium induced failure of inactivation. *Neuron 6*: 691-626, 1991.

Cifelli C, Bourassa F, Gariépy L, Banas K, Benkhalti M, & Renaud JM. KATP channel deficiency in mouse FDB causes fiber damage and impairs Ca2+ release and force development during fatigue in vitro. *J Physiol* (Lond ) 582:843-857,2007

Clausen T, Wang PH, Orskov H, &Kristensen O. Hyperkalemic periodic paralysis: Relationships between changes in plasma water, electrolytes, insulin and catecholamines during attacks. *Scand J Clin Lab Inves*t 40:211-220,1980

Cummins TR &SigworthFJ.Impaired slow inactivation in mutant sodium channels.*Biophys J* 71:227-236, 1996

Cummins TR, Zhou J, Sigworth FJ, Ukomadu C, Stephan M, Ptácek LJ, & Agnew WS.

Functional consequences of a Na+ channel mutation causing hyperkalemic periodic paralysis. *Neuron 10*:667-678,1993

Davies, NP, Eunson, LH, Samuel, M, Hanna, MG. Sodium channel gene mutations in hypokalemic periodic paralysis: an uncommon cause in the UK. *Neurology* 57:1323-1325, 2001.

Duclohier, H. Structure-function studies on the voltage gated sodium channel. *BiochimicaetBiophysicaActa*1788: 2374-2379, 2009

Fakler B, Brandle U, Glowatzki E, Weidmann S, Zenner HP, &Ruppersberg JP .

Strong voltage-dependent inward rectification of inward rectifier K+ channels is caused by intracellular spermine. *Cell 80*:149-154,1995

Featherstone, DE, Richmond, JE, Ruben, PC.Interaction between fast and slow inactivation in Skm1 sodium channels.*Biophys. J.* 71: 3098-3109, 1996.

Fontaine B, Khurana TS, Hoffman EP, Bruns GAP, Haines JL, Trofatter JA, Hanson MP, Rich J, McFarlane H, Yasek DM, Romano D, Gusella JF, and Brown RH. Hyperkalemic periodic paralysis and the adult muscle sodium channel a-subunit gene. *Science* 250: 1000-1002, 1990.

Fozzard, H. A. and Hanck, D. A. Structure and function of voltage-dependent sodium channels: comparison of brain II and Cardiac isoforms. *Physiol. Rev.* 76, 887–926, 1996

Frankenhaeuser B. and A. L. Hodgkin.The action of calcium on the electrical properties of squid axons. *J.Physiol.(Lond.)* 137:218-244, 1957.

Gamstrop I, Hauge M, Helweg – Larsen HF, Mjones H and Sagild U. Adynamiaepisodicahereditaria.A disease clinically resembling familial periodic paralysis but characterized by increasing serum potassium during the paralytic attacks.*Am J Med* 23: 385-390, 1957.

George AL. Inherited disorders of voltage gated sodium channels. *The Journal of Clinical Investigation* 115: 8, 1990-1999, 2005.

Gellens, ME, George, AL, Chen, L, Chahine, M, Horn, R, Barchi, RL, and Kallen RG. Primary structure and functional expression of the human cardiac tetrodotoxin insensitive voltage dependent sodium channel. *Proc. Natl. Acad. Sct* 89: 554 – 558, 1992.

Gissel H and Clausen T. Excitation induced ca2+ influx in rat soleus and edl muscle mechanisms and effects on cellular integrity.*Regulatory and integrative physiology* 279:3.R917-R924,2000

Goldin, AL. Accessory subunits and sodium channel inactivation. *Curr.Opin.Neurobiol.*3:272-277, 1993.

Groome, JR, Fujimoto, E, Ruben, PC. The delay in recovery from fast inactivation in skeletal muscle sodium channels is deactivation. *Cell.Mol.Neurobiol*20: 521-527, 2000.

Guy, HR, Durell, SR. Using sequence homology to analyze the structure and function of voltage gated ion channel proteins. *Soc. Gen. Physiol. Ser.* 49: 197-212, 1994.

Hayward LJ, Sandoval GM and Cannon SC. Defective slow inactivation of sodium channels contribute to familial periodic paralysis. *Neurology* 52: 1447-1453, 1999.

Hayward LJ, Brown RH, & Cannon SC. Inactivation defects caused by myotonia associated mutations in the sodium channel III-IV linker. *J Gen Physio*l 107:559-576, 1997.

Hayward LJ, Kim JS, Lee M-Y, Zhou H, Kim.J.W.,Misra K, Salajegheh M, Wu F-F, Matsuda C, Reid V, Cros D, Hoffman EP, Renaud JM, Cannon SC and Brown RH.Targeted mutation of mouse NaV1.4 muscle sodium channel produces myotonia and potassium sensitive weakness. *J Clin Invest,*2008.

Isom LL. Sodium channel beta subunits: anything but auxiliary. *Neuroscientist.* 7: 42-54, 2001.

Isom, LL, Catterall, WA. Na+ channel subunits and Ig domains. *Nature* 383:307-308, 1996.

Isom, LL, DeJongh, KS, Catterall, WA. Auxiliary subunits of voltage gated ion channels. *Neuron* 12: 1183 – 1194,1994.

Jurkat-Rott K and Lehmann – Horn F. Genotype – phenotype correlation and therapeutic rationale in hyperkalemic periodic paralysis. *Neurotherapeutics* 4: 216-224, 2007.

Koopman, TT, Bezzina, CR, Wilde, AAM. Voltage gated sodium channels: action players with many faces. *Annals of medicine* 38: 472-482, 2006.

Lehmann-Horn F &Jurkat-Rott K. Voltage-gated ion channels and hereditary disease.

*Physiol Rev* 79:1317-1372,1999.

Lehmann – Horn F, Rudel R, Ricker K, Lorkovic H, Dengler R, and Hopf HC. Two cases of adynamiaepisodicahereditaria: an in vitro investigation of muscle cell membrane and contraction parameters. *Muscle Nerve* 6: 113-121, 2007.

Lindinger MI, andHeigenhauser GJ. Ion fluxes during tetanic stimulation in isolated perfused rat hindlimb. *Am J Physiol Regulatory Integrative Comp Physiol* 254: 117-126, 1988.

Marieb, EN, Hoehn, K. Human Anatomy and Physiology.*Benjamin Cummings* 7th edition, 2006.

Mickus, T, Jung, HY, Spruston, N. Properties of slow cumulative sodium channel inactivation in rat hippocampal CA1 pyramidal neurons.*Biophys. J*.76: 846-860, 1999.

Miller TC, da Silva D, Miller HA, Kwiecinski H, Mendell JR, Tawil R, McManis P, Griggs RC, Angelini C, Servidei S, Petajan J, Dalakas MC, Ranum LPW, Fu YH, and Ptacek LJ. Correlating phenotype and genotype in the periodic paralyses.*Neurology*63: 1647-1655, 2004.

Motoike, HK, Liu, H, Glaaser, IW, Yang, AS, Tateyama, M, Kass, RS. The Na+ channel inactivation gate is a molecular comples: a novel role of the COOH terminal domain. *J. Gen. Physiol.* 123:155-65, 2004.

Nakai J, Tanabe T, Konno T, Adams B, Beam KG. Localization in the II-III loop of the dihydropyridine receptor of a sequence critical for excitation contraction coupling. *The Journal of Biological Chemistry*.273: 39:24983-24986,1998.

Nakai J, Sekiguchi N, Rando T, Allen PD, Beam KG. Two regions of the ryanodine receptor involved in coupling with l-type Ca2+ channels. *The Journal of Biological Chemistry*. 273: 13403-13406,1998.

Pearson CL. The periodic paralyses: differential features and pathological observations in permanent myopathic weakness. *Brain* 87: 341-354, 1964.

Rogart, RB, Cribbs, LL, Muglia, LK, Kephart, DD and Kaiser, MW. Molecular cloning of a putative tetrodotoxin resistant rat heart Na+ channel isoform.*Proc. Natl. Acad. Sci*86: 8170-8174,1989.

Rojas, C, Neely A, Velasco-Loyden G, Palma V and Manuel Kukuljan. Hyperkalemic periodic paralysis M1592V mutation modifies activation in human skeletal muscle Na + channel.*Am J Physiol Cell Physiol*276:C259-C266, 1999.

Ruff, RL. Slow inactivation: slow but not dull. *Neurology* 70: 746-747. 2008

Sato, C, Sato, M, Iwasaki, A, Doi, T, Engel, A. The sodium channel has four domains surrounding a central pore. *J. Struct. Biol.* 121: 314-325, 1998.

Streeten DHP, Dalakos TG and Fellerman H. Studies on Hyperkalemic periodic paralysis. Evidence of changes in plasma Na and Cl and induction of paralysis by adrenal glucocorticoids.*JClin Invest* 50: 142- 155, 1971.

Stuhmer, W, Conti, F, Suzuki, H, Wang, XD, Noda, M, Yahagi, N, Kubo,H, Numa, S. Structural parts involved in activation and inactivation of the sodium channel. *Nature* 339: 391-401, 1997.

Sugiura, Y, Aoki, T, Sugiyama, Y, Hida, C, Ogata, M, Yamamoto, T. Temperature sensitive sodium channelopathy with heat induced myotonia and cold induced paralysis. *Neurology* 54: 2179-2181, 2000.

Toib, A, Lyakhov, V, Marom, S. Interaction between duration of activity and time course of recorvery from slow inactivation in mammalian brain Na+ channels. *J. Neurosc.* 18: 1893-1903, 1998.

Ulbricht, W. Sodium channel inactivation: molecular determinants and modulation. *Physiol. Rev.* 85: 1271-1301, 2005.

Vicart, S, Sternberg, D, Fontaine, B, Meola, G. Human skeletal muscle sodium channelopathies. *NeurolSci* 26: 194-202, 2005.

VilinYY, and PC Ruben. Slow inactivation in voltage gated sodium channels. *Cell Biochemistry and Biophysics* 35: 171-191, 2001.

Vilin, YY, Fujimoto, E, Ruben, PC. A single residue differentiates between human cardiac and skeletal muscle Na+ channel slow inactivation. *Biophys. J.* 80: 2221-2230, 2001.

Wang P., Clausen T. Treatment of attacks in hyperkalaemic familial periodic paralysis by inhalation of salbutamol. *Lancet* 307:221–223. 1976.

Whitaker, WR, et al. Distribution of voltage gated sodium channel alpha – subunit and beta subunit mRNAs in human hippocampal formation, cortex and cerebellum. *J. Comp. Neurol,* 422: 123-139, 2000.

Woodhull A. M. Ionic blockage of sodium channels in nerve. *J.Gen.Physiol.* 61:687-708, 1973.

Yensen C, Matar W, & Renaud JM. The K+-induced twitch potentiation is not due to longer action potential. *Am J Physiol* 283:C169-C177,2002.

Yu FH &Catterall WA. Overview of the voltage-gated sodium channel family. *Genome Biology* 4:207-215,2003.

# CHAPTER 6: APPENDICES

## I.

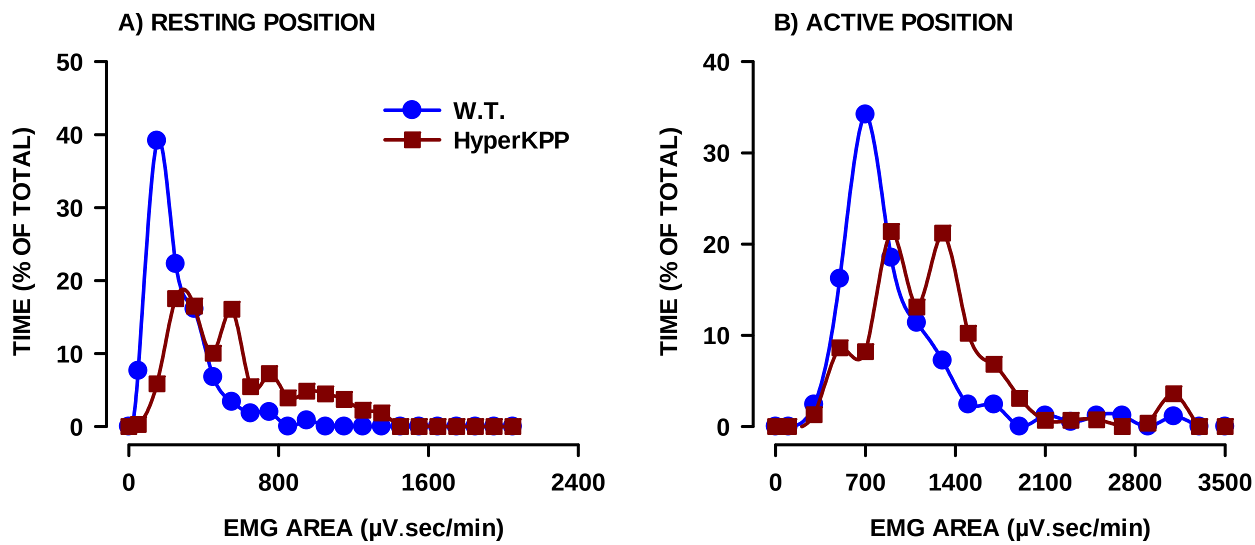


**Figure 6-1.Frequency distribution of the rate of increase of the area under the EMG curve is shifted towards larger values in HyperKPP mice for both A) resting and B) active mice.** Here, 800 ms traces were used instead of the continuous recording system used in the results section. This preliminary measurement showed very similar results as with continuous recording, with HyperKPP mice having larger frequencies of larger slope values. N= 5 for HyperKPP, 2 for WT.

**II.**

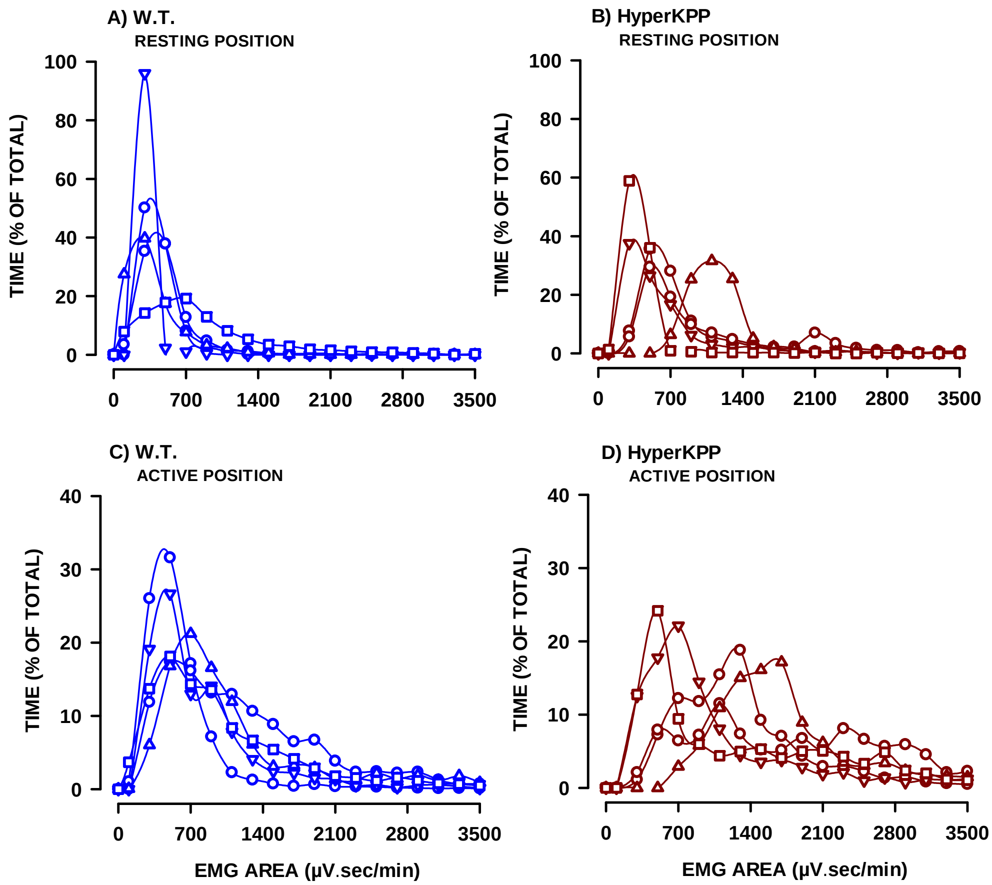


**Figure 6-2.Frequency distribution of the rate of increase of the area under the EMG curve for each animal tested shows large degrees of variability, especially in HyperKPP animals (B and D).** Each animal tested is shown as a separate line on the appropriate panel. There is greater variability between animals tested in HyperKPP afflicted mice.